Quantifying the attenuation of the ketamine phMRI response in humans: a validation using antipsychotic and glutamatergic agents.

O.M. Doyle PhD**, S. De Simoni** MSc**, A.J. Schwarz** PhD**, C. Brittain** MSc**, O.G. O'Daly** PhD**, S.C.R Williams** PhD **and M.A. Mehta** PhD**.**

King's College London, Department of Neuroimaging, Institute of Psychiatry (PO89), De Crespigny Park, London SE5 8AF, UK; OMD, SDS, OGD, SCRW, MAM.

Translational Medicine, Eli Lilly and Company, Indianapolis, Indiana, USA; AJS

Department of Psychological and Brain Sciences, Indiana University, Bloomington, Indiana, USA; AJS.

Statistics, Eli Lilly and Company, Surrey, UK; CB

JPET Fast Forward. Published on January 31, 2013 as DOI: 10.1124/jpet.112.201665
This article has not been copyedited and formatted. The final version may differ from this version.

Running Title**: Modulation of the phMRI response to ketamine.**

Corresponding author: Orla M. Doyle. Department of Neuroimaging, Institute of Psychiatry (PO89), De Crespigny Park, London SE5 8AF, UK.

E-mail: orla.doyle@kcl.ac.uk. Tel: +44 20 3228 3066 Fax: +44 20 3228 2116

Number of text pages: 17

Number of words: abstract - 245,

Number of words: introduction - 689

Number of words: discussion - 1063

Number of figures: 5

Number of tables: 4

Number of references: 45

Abbreviations: 5-HT_{2A} - serotonin 2A, 2-DG - 2-deoxyglucose , AUC – area under the curve, BOLD - blood oxygen level-dependent, CADSS - clinician administered dissociative states scales, EPI – echo planar imaging, FDG-PET - fluorodeoxyglucose positron emission tomography, GPC – Gaussian process classification, LAM-KET – lamotrigine followed by ketamine infusion, MRI – magnetic resonance imaging, NMDA - N-methyl D-aspartate, PCP -phencyclidine, PD – pharmacodynamic, phMRI – pharmacological MRI, PK – pharmacokinetic, PLA-SAL – placebo followed by ketamine infusion, PLA-KET – placebo followed by ketamine infusion, RIS-KET – risperidone followed by ketamine infusion, ROI – regions of interest,

JPET Fast Forward. Published on January 31, 2013 as DOI: 10.1124/jpet.112.201665
This article has not been copyedited and formatted. The final version may differ from this version.

Abstract:

Ketamine acts as an N-methyl D-aspartate (NMDA) receptor antagonist and evokes psychotomimetic symptoms resembling schizophrenia in healthy humans. Imaging markers of acute ketamine challenge have the potential to provide a powerful assay of novel therapies for psychiatric illness, although to date this assay has not been fully validated in humans. Pharmacological magnetic resonance imaging (phMRI) was conducted in a randomised, placebo-controlled cross-over design in healthy volunteers. The study comprised a control and three ketamine infusion sessions, two of which included pre-treatment with lamotrigine or risperidone, compounds hypothesised to reduce ketamine-induced glutamate release. The modulation of the ketamine phMRI response was investigated using univariate analysis of pre-specified regions and a novel application of multivariate analysis across the whole-brain response. Lamotrigine and risperidone resulted in widespread attenuation of the ketamine-induced increases in signal, including frontal and thalamic regions. A contrasting effect across both pre-treatments was observed only in the subgenual prefrontal cortex, for which ketamine produced a reduction in signal. Multivariate techniques proved successful in both classifying ketamine from placebo (100%) and identifying the probability of scans belonging to the ketamine class: ketamine pre-treated with placebo - 0.89. Following pre-treatment these predictive probabilities were reduced to 0.58 and 0.49 for lamotrigine and risperidone, respectively. We have provided clear demonstration of a ketamine phMRI response and its attenuation with both lamotrigine and risperidone. The analytical methodology used could be readily applied to investigate the mechanistic action of novel compounds relevant for psychiatric disorders such as schizophrenia and depression.

JPET Fast Forward. Published on January 31, 2013 as DOI: 10.1124/jpet.112.201665
This article has not been copyedited and formatted. The final version may differ from this version.

Introduction

N-methyl-d-aspartate (NMDA) antagonists induce symptoms resembling schizophrenia in healthy humans, supporting their use as a model to study the role of the glutamate system in psychoses (Farber et al., 1995; Duncan et al., 2000). Ketamine, especially, has been widely used to investigate the role of glutamatergic dysfunction in humans, with acute challenge at sub-anaesthetic doses inducing positive and negative symptoms and impairing cognition (Krystal et al., 1994; Morgan et al., 2004). Across different species and modalities, neuroimaging markers also show robust ketamine-induced changes (Vollenweider et al., 1997; Duncan et al., 1998b; Langsjo et al., 2004; Deakin et al., 2008; Chin et al., 2011; De Simoni et al., 2012; Stone et al., 2012).

Imaging markers of acute ketamine challenge are sensitive to modulation by pre-treatment with antipsychotics and compounds which reduce glutamate transmission. In animals, the antipsychotics clozapine and olanzapine, the anticonvulsant lamotrigine and metabotropic glutamate (mGlu)2/3 receptor agonists or potentiators all attenuate the effects of ketamine or another NMDA antagonist, phencyclidine (PCP), on markers of brain activity (Duncan et al., 1998a; Duncan et al., 2000; Lorrain et al., 2003; Gozzi et al., 2008; Hackler et al., 2010; Chin et al., 2011). In humans, one study to date has demonstrated modulation of the central response to ketamine challenge using neuroimaging (Deakin et al., 2008). Specifically, ketamine was infused intravenously during a resting-state pharmacological MRI (phMRI) timeseries in order to directly measure the compound's effects on the regional blood oxygen level-dependent (BOLD) signal. The BOLD phMRI response to ketamine was attenuated by pre-treatment with a single dose of lamotrigine (Deakin et al., 2008). Ketamine-induced increases in the clinician administered dissociative states scales (CADSS) and brief psychosis rating scales were also reduced by lamotrigine, a finding consistent with a previous behavioural study (Anand et al., 2000). Given that lamotrigine inhibits the release of glutamate, it was concluded that the ketamine-induced change in both symptoms and BOLD

JPET Fast Forward. Published on January 31, 2013 as DOI: 10.1124/jpet.112.201665
This article has not been copyedited and formatted. The final version may differ from this version.

signal (attenuated by lamotrigine) were due to an increase in glutamate release. This is consistent with rodent studies showing increased glutamate efflux in the prefrontal cortex upon acute administration of PCP (Moghaddam et al., 1997) and ketamine (Lorrain et al., 2003); interestingly, both these studies also demonstrated reversal of this glutamate efflux by pre-treatment with mGlu2/3 agonists, presumed to attenuate synaptic glutamate release. Additionally, in humans the link between ketamine administration and cortical glutamate levels has recently been confirmed using magnetic resonance spectroscopy of the anterior cingulate gyrus (Stone et al., 2012) .

In an open-label study, we recently replicated the BOLD phMRI response to ketamine in healthy humans using a sub-anaesthetic dose demonstrating both group-level reproducibility and within-subject reliability (De Simoni et al., 2012). The aims of the present study were to (1) replicate the attenuation of the ketamine-induced BOLD phMRI signal changes using lamotrigine, using a placebo-controlled, repeated-measures design in which all subjects receive treatments; (2) further validate the modulation of the ketamine-induced BOLD signal changes using an existing antipsychotic with a mechanism likely to modulate glutamate release and (3) develop an analysis framework to benchmark the degree of attenuation of ketamine-induced BOLD signal changes. For aim (2), we selected the atypical antipsychotic risperidone, which has high affinities for dopamine D_2 and serotonin 2A (5-HT_{2A}) receptors. Risperidone achieves dopamine D_2 receptor occupancy in the range of clinical efficacy (>50%), whilst being well-tolerated, after a single dose in healthy volunteers (Tauscher et al., 2004) and consistently achieves higher cortical occupancy of 5-HT_{2A} receptors (Farde et al., 1995; Nyberg et al., 1999). 5-HT_{2A} receptor antagonists are hypothesised to contribute to reductions in glutamate release in the cortex, in turn contributing to therapeutic efficacy in psychoses (Large, 2007). We thus expected risperidone to attenuate the effects of ketamine via this 5-HT_{2A}-antagonism (Meltzer et al., 2011).

JPET Fast Forward. Published on January 31, 2013 as DOI: 10.1124/jpet.112.201665
This article has not been copyedited and formatted. The final version may differ from this version.

Using conventional univariate statistics, we tested the modulatory effects in pre-selected regions of interest (ROIs) previously determined to show strong BOLD signal changes in response to ketamine administration (Deakin et al., 2008; De Simoni et al., 2012). Alternatively, pattern recognition approaches, which have not previously been evaluated in the context of resting-state phMRI may be particularly useful because they (1) do not require ROI selection, (2) may be more sensitive than univariate approaches when the pharmacological intervention elicits correlated, distributed effects across brain regions, and (3) reduce effects across brain regions to a *single* outcome measure based on the whole-brain pattern. This framework may have particular value for *in vivo* investigations in which participants are exposed to multiple sessions with different drug regimens, allowing the assessment of the mechanisms of action drugs and their interactions with other compounds at a systems-level.

Here, we build on our previous demonstration of a reliable ketamine phMRI response (De Simoni et al., 2012). Within a placebo-controlled design we seek to replicate the reported attenuation of the ketamine effect by lamotrigine (Deakin et al., 2008) and investigate the effect of pre-treatment with risperidone using both a univariate analysis and a bespoke multivariate framework. Based on previous studies (Anand et al., 2000; Large et al., 2005; Deakin et al., 2008; Gozzi et al., 2008; Meltzer et al., 2011), we expected that both lamotrigine and risperidone would attenuate the effects of ketamine on BOLD phMRI signal through glutamatergic modulation, albeit via different mechanisms of action.

Materials and Methods

Participants

JPET Fast Forward. Published on January 31, 2013 as DOI: 10.1124/jpet.112.201665
This article has not been copyedited and formatted. The final version may differ from this version.

Healthy male volunteers were recruited via advertisements and our volunteer database. Participants were screened for any history of psychiatric, neurological or physical illness. Other exclusion criteria included: positive urine screen for drugs of abuse, out of range urinalysis or standard safety blood test results, consuming of the equivalent >5 caffeinated drinks per day, smoking >5 cigarettes per day or taking prescribed or non-prescribed drugs. Following screening, 20 subjects entered the study. One volunteer withdrew after fainting upon cannulation (session 1), one withdrew due to nausea (session 3) and two others were withdrawn due to positive drug screening. 16 participants (mean age 25.8 years; SD = 5.7; range 20-37) completed all four sessions. All participants gave written informed consent. The study was approved by Wandsworth Research Ethics Committee (09/H0803/48).

Experimental Design

This randomised placebo-controlled, partial crossover design involved screening and four scanning visits. Scanning visits were separated by at least 10 days, this being >5x the longest plasma half-life ($T_{1/2}$) of the two orally-administered compounds where $T_{1/2}$= 35 hours for lamotrigine (Cohen et al., 1987) and $T_{1/2}$ = 20 hours for risperidone (Huang et al., 1993). The T_{max} values for lamotrigine and risperidone were 1-2 hours and 1.4 - 4.8 hours, respectively.

Each visit, participants received a single oral dose of placebo or a study drug and a ketamine or saline infusion (both double-blind). The four combinations administered were: placebo (ascorbic acid) and saline infusion ("PLA-SAL"), placebo and ketamine infusion ("PLA-KET"), lamotrigine (300mg) and ketamine infusion ("LAM-KET") and risperidone (2mg) and ketamine infusion ("RIS-KET"). Treatment order was randomised and balanced within a Latin-square design. The study day timeline is given in Figure 1, with the imaging procedures performed during the broad maximum plasma exposure of both risperidone and lamotrigine (Cohen et al., 1987; Huang et al., 1993). Here, we report the results of the phMRI data only.

JPET Fast Forward. Published on January 31, 2013 as DOI: 10.1124/jpet.112.201665
This article has not been copyedited and formatted. The final version may differ from this version.

Blood samples were taken at 0.5, 1, 1.5, 4 and 8 hours following oral drug administration to determine the plasma pharmacokinetics of lamotrigine or risperidone, and at 15 and 75 minutes after commencing ketamine infusion to confirm target ketamine plasma levels. Heart rate and blood pressure measurements can be found in the supplementary materials (Table S1). Subjective rating scales were also recorded.

Ketamine infusion

Racemic ketamine (Ketalar, Pfizer) was administered intravenously based on the Clements 250 model (Absalom et al., 2007) and implemented in Stanpump (http://anesthesia.standford.edu/pkpd/) using a Graseby 3400 pump with a target plasma level of 75ng/mL in accordance with the subject's height and weight (measured each visit). The sub-anaesthetic dose of ketamine delivered was (mean ± SD) 0.12 ± 0.003 mg/kg during the first minute followed by a pseudo-continuous infusion of approximately 0.31 mg/kg/h. This infusion paradigm was established in an independent cohort as inducing low levels of subjective effects, whilst eliciting a reliable phMRI response (De Simoni et al., 2012).

Subjective Ratings

Subjective effects of ketamine were captured using a brief questionnaire, designed for rapid assessment, administered approximately 4h and 5h post oral dosing (just prior to ketamine infusion and approximately 20 min following initiation of ketamine infusion). The six items in this questionnaire were based on items from the Psychotomimetic States Inventory (PSI), CADSS and visual analogue scales (VAS) that demonstrated high and reliable sensitivity to the administration of ketamine in a separate cohort (De Simoni et al., 2012); see Table S2, supplementary material.

Image Acquisition

JPET Fast Forward. Published on January 31, 2013 as DOI: 10.1124/jpet.112.201665
This article has not been copyedited and formatted. The final version may differ from this version.

Participants were scanned using a 3.0T General Electric Signa HDx scanner. A 15-minute eyes-open resting-state BOLD phMRI scan was acquired using gradient-echo echo-planar imaging (EPI). 450 image volumes of 38 near-axial slices (3mm thickness, interslice gap of 0.3mm aligned to the AC-PC) were acquired per session (TE/TR = 30/2000ms, flip angle (FA) = 75°, in-plane resolution = 3.3mm, matrix size = 64×64, field of view = 21.1 x 21.1cm). A higher resolution gradient echo scan was also acquired (43 3mm-thick near-axial slices with 0.3mm gap, TE/TR = 30/2000ms, FA = 90°, in-plane resolution = 3.3mm, matrix size = 128 x 128, field of view = 24 x 24 cm).

Image pre-processing and modelling

PhMRI data were preprocessed using SPM5 (www.fil.ion.ucl.ac.uk/spm). This involved slice-timing correction, realignment, co-registration to the high-resolution image, spatial normalisation to the SPM EPI template using parameters derived from non-linear normalization of the high-resolution image, and spatial smoothing (8mm FWHM Gaussian kernel). A high-pass filter with a cut-off of 1200s (twice the post infusion phMRI scan duration) was applied to the data to minimise the influence of very low frequency noise and scanner drift.

First-level modelling was performed in a general linear model framework; the design matrix for which was determined in a previous study to reliably capture the ketamine phMRI response (De Simoni et al., 2012). This design matrix comprised the following regressors:

(1) a gamma-variate (GV) function (Madsen, 1992) to model the phMRI response to ketamine;

$$f(t) = \left(\frac{t}{t_{\max}}\right)^{t_{\max}\beta} e^{(t_{\max} - t)\beta}$$

JPET Fast Forward. Published on January 31, 2013 as DOI: 10.1124/jpet.112.201665
This article has not been copyedited and formatted. The final version may differ from this version.

where t_{max} (set to 120, i.e. 240 seconds) relates to the time of the peak amplitude and β (set to 0.01) is a 'shape' parameter. This was preceded by a flat baseline modelling pre-infusion (De Simoni et al., 2012).

(2) the first component of a singular value decomposition of the 6 head motion traces, and

(3) a linear drift term.

The beta images from the contrast of the first regressor were used in the group-level analyses.

Group-level Univariate Analysis

Atlas- and coordinate-based ROIs responsive to ketamine were pre-specified based on previous studies (Deakin et al., 2008; De Simoni et al., 2012) (supplementary material). These included the anterior cingulate cortex, supragenual paracingulate cortex, thalamus, posterior cingulate cortex, supplementary motor area, left anterior insula, right anterior insula, left operculum, right operculum, precuneus and medial occipital lobes. Mean beta values were extracted from each ROI with MarsBar (Brett et al., 2002) from the first-level beta maps.

Statistical analysis of the ROI measures was performed in SAS v.9.1 (www.sas.com) using a mixed effects model with treatment (fixed), session (fixed), ROI (fixed) and subject (random) as factors. Mean estimates for each treatment condition and the mean differences between treatment conditions, across ROIs, were generated for the following comparisons: PLA-KET vs. LAM-KET; PLA-KET vs. RIS-KET; and PLA-SAL vs. PLA-KET. Post-hoc comparisons by ROI were performed using analogous models.

Whole-brain univariate analyses were also performed using flexible factorial ANOVA models in SPM with a statistical significance threshold of $p<0.05$ (cluster corrected with $p<0.001$ voxelwise threshold).

Group-level Multivariate Analysis

JPET Fast Forward. Published on January 31, 2013 as DOI: 10.1124/jpet.112.201665
This article has not been copyedited and formatted. The final version may differ from this version.

We used Gaussian process classification (GPC), a probabilistic approach to classification that models the posterior probabilities of a class label [1, -1] for an unseen test sample, given a set of training data (Rasmussen et al., 2006). For example, on training the GPC with a subset of the PLA-KET images (label: 1) and PLA-SAL images (label: -1), the GPC can then predict the probability of an unseen image belonging to the PLA-KET group while capturing the confidence of the predicted label. This is particularly useful for pharmacological modulation applications (Marquand et al., 2010) as it enables us to place an individual phMRI response on a continuum to gauge the extent of the modulation relative to a control condition (PLA-KET in this case). To assign a categorical label to an unseen test case the predictive probability was thresholded at 0.5. A detailed account of GPC is provided in the supplementary material.

Implementation of Gaussian process classification.

Given the repeated measures nature of this study, the GPC was trained in a leave-one-out manner whereby data from 15 of the participants were used to train the model and the final (unseen) participant's data were used for testing. Additionally, the beta images were mean-centred (prior to classification) in a within-subject manner by subtracting from each voxel the mean across the contrast of interest images (e.g. for classification against the PLA-SAL - PLA-KET continuum the mean per voxel of the PLA-SAL and PLA-KET conditions was subtracted from the images for all four conditions (Figure 2).

Statistical significance of the classification accuracies were assessed using permutation testing. The class labels were randomly permuted 1000 times and the classifier was re-trained using these labels to create a probability distribution of the accuracy.

Two group-level contrasts were investigated using the classifier:

JPET Fast Forward. Published on January 31, 2013 as DOI: 10.1124/jpet.112.201665
This article has not been copyedited and formatted. The final version may differ from this version.

1. The classifier was trained on PLA-SAL and PLA-KET images and then tested on all 4 conditions for the remaining unseen subject. This allowed the RIS-KET and LAM-KET scans to be positioned on the PLA-SAL – PLA-KET continuum.
2. The classifier was trained on the LAM-KET (or RIS-KET) and PLA-KET images and tested only on the corresponding LAM-KET (or RIS-KET) and PLA-KET from the unseen subject. This directly tested the modulation of the ketamine response by lamotrigine (or risperidone) in the absence of the PLA-SAL infusion scans.

Multivariate maps (g-maps) were constructed to visualise the spatial pattern driving the classification. For the g-map, training samples contribute in proportion to how representative they are of their respective class (Marquand et al., 2010). Since multivariate techniques are sensitive to spatial correlation, and the performance of the classifier is based on the entire pattern rather than individual voxels, inference based on local regions should be avoided when interpreting these maps. See supplementary materials.

Results

Pharmacokinetics

The mean and standard deviation of plasma concentration of ketamine per-treatment was (in ng/mL): PLA-KET 62.7 ± 17.6, LAM-KET 66.1 ± 22.1 and RIS-KET 49.1 ± 15.9 after 15 minutes of infusion (concentration of KET was significantly different for RIS-KET compared to PLA-KET, p=0.02, Wilcoxon rank sum), and PLA-KET 72.8 ± 20.8, LAM-KET 71.9 ± 35.5 and RIS-KET 77.8 ± 26.9 after 75 minutes of infusion. Maximum risperidone concentrations were achieved between 1 and 4.5 hours post-dose (median of 2 hours). Geometric mean (geometric percent coefficient of variation) area under the curve (AUC)[0-4.5hr] and AUC[0-8hr] estimates of risperidone concentration were 40.0 (79) and 61.7 (83) ng.hr/mL, respectively. Similarly, maximum lamotrigine concentrations were achieved

JPET Fast Forward. Published on January 31, 2013 as DOI: 10.1124/jpet.112.201665
This article has not been copyedited and formatted. The final version may differ from this version.

between 1 and 4.5 hours post-dose (median of 1.75 hours). Geometric mean AUC[0-4.5hr] and AUC[0-8hr] estimates of lamotrigine concentration were 14,125 (16) and 26,018 (17) ng.hr/mL, respectively. The pharmacokinetic profile of both compounds described a broad plateau following T_{max}, consistent with previously described elimination times.

Univariate analysis

The ROI analysis revealed a significant BOLD response to ketamine infusion, relative to saline ($p<0.001$; Tables 1-3). This included both positive (Tables 1, 2) and negative (Table 3) BOLD changes. For the positively-responding regions, pre-treatment with both lamotrigine and risperidone resulted in a relatively consistent attenuation of the ketamine responses intermediate between the PLA-SAL and PLA-KET conditions ($p<0.001$ for both lamotrigine and risperidone) (Figure 3 (a,c)). BOLD timeseries from two ROIs which are representative of all the positively responding regions are shown in Figure 4. For the negatively-responding regions in the subgenual cingulate and ventromedial prefrontal cortex, risperidone strongly attenuated the negative BOLD response ($p<0.001$) whereas the effect of lamotrigine was weaker ($p=0.046$). Only this region differed between the pre-treatment conditions ($p = 0.042$). In the striatum, neither risperidone nor lamotrigine attenuated the response to ketamine (post hoc t-tests; $p>0.15$). Whole-brain maps of PLA-SAL contrasted with PLA-KET, and PLA_KET contrasted with both LAM-KET and RIS-KET are provided in the supplementary materials (Figure S2).

Multivariate whole-brain analysis

The GPC was applied to the whole-brain beta images to provide categorical classification labels, i.e. PLA-SAL or PLA-KET, and predictive probabilities of KET infusion. The classifier was initially trained on the PLA-SAL vs. PLA-KET condition and then tested on all four conditions for the unseen subject, see Table 4. Perfect classification (100%) was

achieved for PLA-SAL versus PLA-KET. Lamotrigine pre-treatment resulted in a reduced accuracy of 87.5% with 4/16 of the subjects in the LAM-KET class being labelled as PLA-SAL. Risperidone pre-treatment also resulted in reduced accuracy (75%) with 8/16 of the subjects in the RIS-KET class being labelled as PLA-SAL.

The mean posterior probabilities of belonging to the PLA-KET group (Figure 5a) showed a marked reduction with both LAM (mean 0.58) and RIS (mean 0.49) pre-treatment. The comparisons between PLA-KET vs. LAM-KET and PLA-KET vs. RIS-KET were both highly significant (Wilcoxon rank sum test, $p = 0.00042$ and $p = 0.00036$ respectively). There was no statistically significant difference between the LAM-KET versus RIS-KET conditions.

In Figure 5b, the PLA-SAL to PLA-KET continuum illustrates an excellent separation between the PLA-SAL and PLA-KET groups with only one subject close to misclassification. The LAM-KET predictive probabilities are widely spread across the continuum (0.10 – 0.97, mean = 0.58), similar to the RIS-KET predictive probabilities (0.01 – 0.90, mean = 0.49). The distributed patterns of brain regions (the g-map) driving the discrimination between PLA-SAL and PLA-KET is illustrated in Figure 6. The g-map shows a striking similarity to the univariate map of the same contrast (Figure S2).

To directly investigate the attenuation of the ketamine response we classified LAM-KET and RIS-KET against PLA-KET. Here, high classification accuracy indicates that the pre-treated scans are dissimilar to the PLA-KET condition. The performance of the classifiers for LAM-KET and RIS-KET conditions versus PLA-KET were significantly above chance ($p<0.05$), 68.8% and 81.3% (see supplementary material), respectively. The g-maps for both models can be seen in the supplementary material (Figure S3 and S4). Both maps appear to be highly similar indicating that the distributed ketamine response was broadly attenuated by both LAM and RIS pre-treatment.

Subjective ratings

JPET Fast Forward. Published on January 31, 2013 as DOI: 10.1124/jpet.112.201665
This article has not been copyedited and formatted. The final version may differ from this version.

Participants reported feeling less alert and clear-headed after ketamine infusion (pre- vs post-infusion). When pre-treated with lamotrigine and risperidone there was no significant effect of ketamine on the alert-drowsy scale, while significant differences remained for the muzzy-clear scale. See supplementary materials.

Correlations between PK and phMRI responses

No significant correlations were found between ketamine plasma levels and either the BOLD phMRI changes or predictive probabilities from the GPC. See supplementary materials.

In order to explore whether the response to risperidone pre-treatment was related to the response to lamotrigine pre-treatment to investigate potential shared mechanistic endpoints, we also tested the correlation between the predictive probabilities of belonging to the ketamine class for the two pre-treatments. A significant correlation was found (Spearman's rho = 0.61, p=0.014).

Discussion

We found that lamotrigine and the antipsychotic risperidone attenuated the phMRI response to ketamine to a similar degree. This was demonstrated using both univariate analyses of predefined ROIs (Deakin et al., 2008; De Simoni et al., 2012) and a novel application of multivariate pattern analysis to the whole-brain phMRI response. The latter approach may have particular value for *in vivo* investigation of mechanisms of action of existing and novel compounds at a systems-level.

In the univariate analysis, lamotrigine and risperidone attenuated the ketamine effect across most ROIs including medial prefrontal and cingulate regions and the thalamus. Using multivariate analysis, the predictive probability of belonging to the ketamine class (without

pre-treatment) was computed across all four conditions. The phMRI response to ketamine is known to be strong (Deakin et al., 2008; De Simoni et al., 2012) and this was reflected in the correct discrimination of *all* placebo-saline from placebo-ketamine conditions, thus providing a robust assay to investigate modulation by pharmacological pre-treatment.

Pre-treatment with either lamotrigine or risperidone resulted in attenuation of the phMRI response to ketamine (benchmarked against the predictive probability of belonging to the ketamine class). Indeed, both lamotrigine and risperidone pre-treatment resulted in phMRI responses to ketamine that were more difficult to separate from the saline condition than ketamine alone. While the accuracies, predictive probabilities and univariate maps (Figure S2) suggested that risperidone was slightly more effective in attenuating the positive ketamine phMRI response, there was no difference when these two conditions were contrasted directly using the GPC (56% accuracy, see supplementary materials) and the predictive probabilities between these two conditions were correlated. ROI analysis showed that only risperidone pre-treatment blocked the subgenual prefrontal cortex response to ketamine, a region that may be important in understanding antidepressant effects of treatments (Agid et al., 2007). Direct comparison between the LAM-KET and RIS-KET responses in these ROIs using post-hoc t-tests revealed a significant difference in the subgenual cingulate with risperidone having the larger effect. Interestingly, the subgenual prefrontal cortex has a particularly high innervation of 5-HT neurons indicated by binding of [3H]citalopram, suggesting serotonergic mechanisms may play a role in the effects of acute ketamine within this region (Mantere et al., 2002; Varnas et al., 2004) and the attenuation of these effects with risperidone. This however remains speculative with formal testing using selective 5-HT2A antagonists required. Overall, this indicates that risperidone and lamotrigine produce a global attenuation of the positive ketamine response in contrast to the selective attenuation with risperidone of the subgenual response.

Lamotrigine is a broad spectrum anticonvulsant that inhibits voltage-gated ion channels, including sodium and calcium, with downstream effects resulting in inhibition of glutamate release (Large et al., 2005). Our findings are in keeping with previous studies in experimental animals and humans. In animals, acute administration of lamotrigine produced widespread inhibition of the relative cerebral blood volume response to the NMDA receptor antagonist PCP in all activated regions (Gozzi et al., 2008). When administered prior to a ketamine challenge in healthy volunteers, lamotrigine has been shown to reverse ketamine's effects on behavioural and cognitive measures (Anand et al., 2000), and reduce the ketamine-induced changes in the BOLD signal (Deakin et al., 2008).

This is the first study to investigate pre-treatment with risperidone on the BOLD signal response to ketamine in healthy volunteers. In addition to its serotonergic effects, risperidone has high affinity for dopamine D2 receptors, which may conceivably have an impact on its interaction with ketamine. However, studies using selective D2 antagonists, such as haloperidol or raclopride, have failed to demonstrate a modulation of the effects of ketamine or PCP (Krystal et al., 1999; Gozzi et al., 2008; Oranje et al., 2009). Furthermore, no effects were observed in the striatum on the ketamine-induced BOLD changes following risperidone. Given the high density of dopamine D2 receptors in the striatum, this supports the proposal that antagonism at 5-HT_{2A} receptors is the prevailing mechanism underlying the risperidone-induced attenuation of the ketamine BOLD response via attenuated glutamate release (Adams and Moghaddam, 1998; Aghajanian and Marek, 2000; Large, 2007). Indeed, 5-HT_{2A} selective antagonists and risperidone itself can block NMDAR antagonist induced deficits in locomotor function (Meltzer et al., 2011), and cognitive function (Varty et al., 1999; Mirjana et al., 2004; Didriksen et al., 2007), deficits thought to be the result of a frontal hyperglutamatergic state.

We cannot preclude that the main effects of lamotrigine and risperidone might influence the measurement of the ketamine response, even though it was derived relative to the pre-infusion

baseline. Given that the BOLD signal is non-quantitative, the pre-infusion baseline cannot be compared directly across conditions, thus further experiments would be required to delineate the main effects of both pre-treatments, using for example dual-echo acquisition which simultaneously acquires BOLD and quantitative perfusion signals (Wong et al., 1997).

Direct pharmacological effects on the vasculature represent a possible confound in the interpretation of our results. However, there are a number of reasons why vascular effects cannot explain our findings. First, the effects of ketamine alone match earlier observations using metabolism markers (2-deoxyglucose (2-DG) autoradiography in the rodent and fluorodeoxyglucose positron emission tomography (FDG-PET) in humans) (Duncan et al., 1998b; Langsjo et al., 2004). Second, we observed both increases and decreases in the BOLD signal response to ketamine, which is difficult to understand in a purely vascular framework. Third, a vascular account would predict differential effects based on the distribution of pharmacological targets. For example, risperidone would be predicted to have a greater effect in areas of high dopamine receptor density such the striatum (dopamine is known to modulate vasodilation and constriction directly (Krimer et al., 1998)). Instead, the observed attenuation of the ketamine-induced response to lamotrigine and risperidone was highly similar.

Another potential limitation is that the plasma levels of ketamine during the risperidone arm were significantly lower than the other study arms in the 15 minute sample. This may be because the enzyme cytochrome P450 3A4, which is known to metabolise both risperidone and ketamine (Fang et al., 1999). Thus, it is possible that the attenuation of the ketamine effect is via an increased enzymatic activity induced by risperidone, resulting in lower delivered dose of ketamine. However, the ketamine levels were assessed after the phMRI scan from which the results were derived. It is not known whether the lower levels would have been present during the administration. Also, an explanation based purely on ketamine

JPET Fast Forward. Published on January 31, 2013 as DOI: 10.1124/jpet.112.201665
This article has not been copyedited and formatted. The final version may differ from this version.

exposure is not supported by the data as the degree of attenuation is not correlated with the plasma levels of ketamine.

Outside of its antagonist activity at NMDA receptors, ketamine also has effects at mu-opioid receptors, acts as an inhibitor at serotonin and noradrenaline reuptake sites, interacts with cholinergic and sigma receptors and affects the dopamine system (Freeman and Bunney, 1984; Schmidt and Fadayel, 1996; Kapur and Seeman, 2002). Such effects have been described at higher doses and in relation to analgesia, although it remains possible that non-NMDA effects contributed towards the changes observed in this study. More selective compounds aimed at modulating glutamate and other systems would be required to fully characterise the ketamine-induced changes in BOLD signal.

Conclusions

We have confirmed robust BOLD signal changes following acute administration of the NMDA antagonist, ketamine, which can create a cluster of symptoms redolent of schizophrenia. Our analysis framework provided clear demonstration of both a ketamine effect when contrasted against placebo, and an attenuation of this response with both lamotrigine and risperidone pre-treatment. Our data also suggest serotonergic mechanisms play a role in the ketamine-induced subgenual cingulate changes, with potential relevance for understanding its antidepressant effects. This extends our previous work showing good reliability of the ketamine phMRI assay (De Simoni et al., 2012) and provides an analytical methodology to investigate the mechanistic action of novel compounds and inform important questions such as dose selection, particularly for those that do not rely on dopamine D_2 receptor blockade.

Acknowledgements

We thank the radiographers and physicists at the Centre for Neuroimaging Sciences for their assistance during this research.

References

Absalom AR, Lee M, Menon DK, Sharar SR, De Smet T, Halliday J, Ogden M, Corlett P, Honey GD and Fletcher PC (2007) Predictive performance of the Domino, Hijazi, and Clements models during low-dose target-controlled ketamine infusions in healthy volunteers. *British journal of anaesthesia* **98**:615-623.

Adams B and Moghaddam B (1998) Corticolimbic dopamine neurotransmission is temporally dissociated from the cognitive and locomotor effects of phencyclidine. *J Neurosci* **18**:5545-5554.

Aghajanian GK and Marek GJ (2000) Serotonin model of schizophrenia: emerging role of glutamate mechanisms. *Brain research Brain research reviews* **31**:302-312.

Agid Y, Buzsaki G, Diamond DM, Frackowiak R, Giedd J, Girault JA, Grace A, Lambert JJ, Manji H, Mayberg H, Popoli M, Prochiantz A, Richter-Levin G, Somogyi P, Spedding M, Svenningsson P and Weinberger D (2007) How can drug discovery for psychiatric disorders be improved? *Nat Rev Drug Discov* **6**:189-201.

Anand A, Charney DS, Oren DA, Berman RM, Hu XS, Cappiello A and Krystal JH (2000) Attenuation of the neuropsychiatric effects of ketamine with

lamotrigine: support for hyperglutamatergic effects of N-methyl-D-aspartate receptor antagonists. *Arch Gen Psychiatry* **57**:270-276.

Brett M, Anton JL, Valabregue R and Poline JB (2002) Region of interest analysis using an SPM toolbox. *NeuroImage* **16**.

Chin CL, Upadhyay J, Marek GJ, Baker SJ, Zhang M, Mezler M, Fox GB and Day M (2011) Awake rat pharmacological magnetic resonance imaging as a translational pharmacodynamic biomarker: metabotropic glutamate 2/3 agonist modulation of ketamine-induced blood oxygenation level dependence signals. *The Journal of pharmacology and experimental therapeutics* **336**:709-715.

Cohen AF, Land GS, Breimer DD, Yuen WC, Winton C and Peck AW (1987) Lamotrigine, a new anticonvulsant: pharmacokinetics in normal humans. *Clinical pharmacology and therapeutics* **42**:535-541.

De Simoni S, Schwarz AJ, O'Daly OD, S. S, Zelaya FO, Williams SCR and Mehta MA (2012) Test-retest reliability of the BOLD pharmacological MRI response to ketamine in healthy volunteers. *NeuroImage* **In press**.

Deakin JF, Lees J, McKie S, Hallak JE, Williams SR and Dursun SM (2008) Glutamate and the neural basis of the subjective effects of ketamine: a pharmaco-magnetic resonance imaging study. *Arch Gen Psychiatry* **65**:154-164.

Didriksen M, Skarsfeldt T and Arnt J (2007) Reversal of PCP-induced learning and memory deficits in the Morris' water maze by sertindole and other antipsychotics. *Psychopharmacology (Berl)* **193**:225-233.

Duncan GE, Leipzig JN, Mailman RB and Lieberman JA (1998a) Differential effects of clozapine and haloperidol on ketamine-induced brain metabolic activation. *Brain Res* **812**:65-75.

Duncan GE, Miyamoto S, Leipzig JN and Lieberman JA (2000) Comparison of the effects of clozapine, risperidone, and olanzapine on ketamine-induced alterations in regional brain metabolism. *J Pharmacol Exp Ther* **293**:8-14.

Duncan GE, Moy SS, Knapp DJ, Mueller RA and Breese GR (1998b) Metabolic mapping of the rat brain after subanesthetic doses of ketamine: potential relevance to schizophrenia. *Brain Res* **787**:181-190.

Fang J, Bourin M and Baker GB (1999) Metabolism of risperidone to 9-hydroxyrisperidone by human cytochromes P450 2D6 and 3A4. *Naunyn-Schmiedeberg's archives of pharmacology* **359**:147-151.

Farber NB, Wozniak DF, Price MT, Labruyere J, Huss J, St Peter H and Olney JW (1995) Age-specific neurotoxicity in the rat associated with NMDA receptor blockade: potential relevance to schizophrenia? *Biological psychiatry* **38**:788-796.

Farde L, Nyberg S, Oxenstierna G, Nakashima Y, Halldin C and Ericsson B (1995) Positron emission tomography studies on D2 and 5-HT2 receptor binding in risperidone-treated schizophrenic patients. *Journal of clinical psychopharmacology* **15**:19S-23S.

Freeman AS and Bunney BS (1984) The effects of phencyclidine and N-allylnormetazocine on midbrain dopamine neuronal activity. *European journal of pharmacology* **104**:287-293.

Gozzi A, Large CH, Schwarz A, Bertani S, Crestan V and Bifone A (2008) Differential effects of antipsychotic and glutamatergic agents on the phMRI response to phencyclidine. *Neuropsychopharmacology* **33**:1690-1703.

Hackler EA, Byun NE, Jones CK, Williams JM, Baheza R, Sengupta S, Grier MD, Avison M, Conn PJ and Gore JC (2010) Selective potentiation of the metabotropic glutamate receptor subtype 2 blocks phencyclidine-induced hyperlocomotion and brain activation. *Neuroscience* **168**:209-218.

Huang ML, Van Peer A, Woestenborghs R, De Coster R, Heykants J, Jansen AA, Zylicz Z, Visscher HW and Jonkman JH (1993) Pharmacokinetics of the novel antipsychotic agent risperidone and the prolactin response in healthy subjects. *Clinical pharmacology and therapeutics* **54**:257-268.

Kapur S and Seeman P (2002) NMDA receptor antagonists ketamine and PCP have direct effects on the dopamine D(2) and serotonin 5-HT(2)receptors-implications for models of schizophrenia. *Mol Psychiatry* **7**:837-844.

Krimer LS, Muly EC, 3rd, Williams GV and Goldman-Rakic PS (1998) Dopaminergic regulation of cerebral cortical microcirculation. *Nat Neurosci* **1**:286-289.

Krystal JH, D'Souza DC, Karper LP, Bennett A, Abi-Dargham A, Abi-Saab D, Cassello K, Bowers MB, Jr., Vegso S, Heninger GR and Charney DS (1999) Interactive effects of subanesthetic ketamine and haloperidol in healthy humans. *Psychopharmacology (Berl)* **145**:193-204.

Krystal JH, Karper LP, Seibyl JP, Freeman GK, Delaney R, Bremner JD, Heninger GR, Bowers MB, Jr. and Charney DS (1994) Subanesthetic effects of the noncompetitive NMDA antagonist, ketamine, in humans. Psychotomimetic, perceptual, cognitive, and neuroendocrine responses. *Arch Gen Psychiatry* **51**:199-214.

Langsjo JW, Salmi E, Kaisti KK, Aalto S, Hinkka S, Aantaa R, Oikonen V, Viljanen T, Kurki T, Silvanto M and Scheinin H (2004) Effects of subanesthetic ketamine on regional cerebral glucose metabolism in humans. *Anesthesiology* **100**:1065-1071.

Large CH (2007) Do NMDA receptor antagonist models of schizophrenia predict the clinical efficacy of antipsychotic drugs? *J Psychopharmacol* **21**:283-301.

Large CH, Webster EL and Goff DC (2005) The potential role of lamotrigine in schizophrenia. *Psychopharmacology (Berl)* **181**:415-436.

Lorrain DS, Baccei CS, Bristow LJ, Anderson JJ and Varney MA (2003) Effects of ketamine and N-methyl-D-aspartate on glutamate and dopamine release in the rat prefrontal cortex: modulation by a group II selective metabotropic glutamate receptor agonist LY379268. *Neuroscience* **117**:697-706.

Madsen MT (1992) A Simplified Formulation of the Gamma Variate Function. *Phys Med Biol* **37**:1597-1600.

Mantere T, Tupala E, Hall H, Sarkioja T, Rasanen P, Bergstrom K, Callaway J and Tiihonen J (2002) Serotonin transporter distribution and density in the

cerebral cortex of alcoholic and nonalcoholic comparison subjects: a whole-hemisphere autoradiography study. *Am J Psychiatry* **159**:599-606.

Marquand A, Howard M, Brammer M, Chu C, Coen S and Mourao-Miranda J (2010) Quantitative prediction of subjective pain intensity from whole-brain fMRI data using Gaussian processes. *NeuroImage* **49**:2178-2189.

Meltzer HY, Horiguchi M and Massey BW (2011) The role of serotonin in the NMDA receptor antagonist models of psychosis and cognitive impairment. *Psychopharmacology (Berl)* **213**:289-305.

Mirjana C, Baviera M, Invernizzi RW and Balducci C (2004) The serotonin 5-HT2A receptors antagonist M100907 prevents impairment in attentional performance by NMDA receptor blockade in the rat prefrontal cortex. *Neuropsychopharmacology* **29**:1637-1647.

Moghaddam B, Adams B, Verma A and Daly D (1997) Activation of glutamatergic neurotransmission by ketamine: a novel step in the pathway from NMDA receptor blockade to dopaminergic and cognitive disruptions associated with the prefrontal cortex. *J Neurosci* **17**:2921-2927.

Morgan CJ, Mofeez A, Brandner B, Bromley L and Curran HV (2004) Acute effects of ketamine on memory systems and psychotic symptoms in healthy volunteers. *Neuropsychopharmacology* **29**:208-218.

Nyberg S, Eriksson B, Oxenstierna G, Halldin C and Farde L (1999) Suggested minimal effective dose of risperidone based on PET-measured D2 and 5-HT2A receptor occupancy in schizophrenic patients. *Am J Psychiatry* **156**:869-875.

Oranje B, Gispen-de Wied CC, Westenberg HG, Kemner C, Verbaten MN and Kahn RS (2009) Haloperidol counteracts the ketamine-induced disruption of processing negativity, but not that of the P300 amplitude. *Int J Neuropsychopharmacol* **12**:823-832.

Rasmussen CE, Williams CKI and Books24x7 Inc. (2006) Gaussian processes for machine learning, in, MIT Press, Cambridge, Mass.

Schmidt CJ and Fadayel GM (1996) Regional effects of MK-801 on dopamine release: effects of competitive NMDA or 5-HT2A receptor blockade. *J Pharmacol Exp Ther* **277**:1541-1549.

Stone JM, Dietrich C, Edden R, Mehta MA, De Simoni S, Reed LJ, Krystal JH, Nutt D and Barker GJ (2012) Ketamine effects on brain GABA and glutamate levels with 1H-MRS: relationship to ketamine-induced psychopathology. *Molecular psychiatry* **17**:664-665.

Tauscher J, Hussain T, Agid O, Verhoeff NPLG, Wilson AA, Houle S, Remington G, Zipursky RB and Kapur S (2004) Equivalent occupancy of dopamine D(1) and D(2) receptors with clozapine: Differentiation from other atypical antipsychotics. *The American journal of psychiatry* **161**:1620-1625.

Varnas K, Halldin C and Hall H (2004) Autoradiographic distribution of serotonin transporters and receptor subtypes in human brain. *Hum Brain Mapp* **22**:246-260.

Varty GB, Bakshi VP and Geyer MA (1999) M100907, a serotonin 5-HT2A receptor antagonist and putative antipsychotic, blocks dizocilpine-induced prepulse inhibition deficits in Sprague-Dawley and Wistar rats. *Neuropsychopharmacology* **20**:311-321.

Vollenweider FX, Leenders KL, Scharfetter C, Antonini A, Maguire P, Missimer J and Angst J (1997) Metabolic hyperfrontality and psychopathology in the ketamine model of psychosis using positron emission tomography (PET) and [18F]fluorodeoxyglucose (FDG). *Eur Neuropsychopharmacol* **7**:9-24.

Wong EC, Buxton RB and Frank LR (1997) Implementation of quantitative perfusion imaging techniques for functional brain mapping using pulsed arterial spin labeling. *NMR Biomed* **10**:237-249.

Data collection was supported by a research grant from Eli Lilly and Company. Data analysis was supported by Eli Lilly and Company and the Innovative Medicines Initiative Joint Undertaking under Grant Agreement No 115008 (NEWMEDS). The Innovative Medicines Initiative Joint Undertaking is a public-private partnership between the European Union and the European Federation of Pharmaceutical Industries and Associations.

Conflict of Interest

Dr. Mitul A. Mehta is a scientific advisor for Cambridge Cognition. Dr. Mitul A. Mehta and Dr. Steve C.R. Williams currently consult for UCB Pharmaceuticals. Dr. Adam J. Schwarz and Claire Brittain are employees and shareholders of Eli Lilly and Company. All other authors declare no conflicts of interest.

Orla M. Doyle and Sara De Simoni contributed equally to this work.

Orla Doyle,
Centre for Neuroimaging Sciences P089,
Institute of Psychiatry,
De Crespigny Park,
London,
SE5 8AF.
Email: orla.doyle@kcl.ac.uk

Authorship Contributions

Participated in research design: De Simoni, Brittain, Schwarz, Mehta, Williams. O'Daly.

Conducted experiments: De Simoni, Mehta,

Contributed new reagents or analytic tools: Doyle.

Performed data analysis: Doyle, De Simoni, Brittain

Wrote or contributed to the writing of the manuscript: Doyle, De Simoni, Schwarz, Brittain, O'Daly, Williams, Mehta.

Legends for figures

Figure 1: Timeline of events on each study day. MRI scans acquired during the oral drug administration phase and infusion phase included cognitive fMRI tasks and a breathold paradigm. Results from these analyses are not reported here. Times are shown in 24 hour clock convention.

Figure 2: Analysis pipeline. 1. Experimental setup. 2. Univariate analysis; incorporating image preprocessing and GLM analysis. 3. Data preparation prior to pattern recognition which exploits the repeated measures design, and 4. Training and testing of the GPC models created per subject and an illustration of the PLA-KET continuum.

Figure 3: Univariate responses by treatment condition for preselected ROIs (mean ± SEM across subjects). The annotation "[Dk]" identifies coordinates specified based on (Deakin et al., 2008) (a) Anatomical ROIs corresponding to brain regions strongly responding to the ketamine challenge. (b) Anatomical ROIs from the dorsal striatum to interrogate any preferential effect of risperidone due to its D2 antagonist properties. (c) Coordinate-based ROIs corresponding to foci of strong response to the ketamine challenge in a preparatory pilot study. (d) Coordinate-based ROIs corresponding to foci of strong negative BOLD responses to the ketamine challenge observed in a separate cohort (De Simoni et al., 2012) and in (Deakin et al., 2008) (Abbreviations: paCC = supragenual paracingulate gyrus; ACC = anterior cingulate cortex; PCC = posterior cingulate cortex; PreC = precuneus; SMA = supplementary motor area; Thal = thalamus; Oper(L) = operculum (left); Oper(R) = operculum (right); Ins(L) = anterior insula (left); Ins(R) = anterior insula (right); MedOcc = medial occipital lobes; Caud = caudate; Put = putamen; MidCC = mid-cingulate cortex; mPFC = medial prefrontal cortex; dlPFC(R) = dorsolateral prefrontal cortex (right); vlPFC(R) = ventrolateral prefrontal cortex (right); phc(L) = parahippocamPLA gyrus (left); phc(R) =

parahippocamPLA gyrus (right); sgCC = subgenual cingulate cortex. See methods for description of ROI definitions.)

Figure4: BOLD signal time courses from posterior cingulate cortex and bilateral operculum (mean ± SEM across subjects for each treatment condition).

Figure 5(a): Posterior probability of belonging to the PLA-KET treatment class for each drug contrast. The probability of belonging to the ketamine class *** - $p<0.001$. **Figure 5**(b): Placebo to Ketamine continuum derived from the output of the GPC. A p(Ket|x*) close to one implies a high probability of belonging to the ketamine class and a p(Ket|x*) close to zero implies high probability of belonging to the placebo class. The y-axis is used to separate the groups into three rows, with some jitter added to each row for visualisation.

Figure6: Multivariate map (g-map) from the GPC which contrasts PLA-KET (class label: +1) and PLA-SAL (class label: -1). A positive g-map coefficient for a particular voxel indicates a higher overall beta score for the PLA-KET class (+1) and similarly, a negative g-map coefficient indicates a higher overall beta score for the PLA-SAL class (-1). The right hand side of each image corresponds to the participants' right side with the transaxial slice numbers in MNI coordinates (z-axis) shown in white.

JPET Fast Forward. Published on January 31, 2013 as DOI: 10.1124/jpet.112.201665
This article has not been copyedited and formatted. The final version may differ from this version.

Table 1: Comparison of LS mean difference across all anatomical ROIs[1,2] (excluding Caudate and Putamen)

			Contrast		
N	**Treatment**	**LS Mean (95% CI)**	**Paired comparison**	**Difference (95% CI)**	**p**
16	PLA-KET	2.4211 (2.0404, 2.8018)	PK – PS	2.5283 (2.2927, 2.7639)	<0.001
16	LAM-KET	1.3788 (0.9981, 1.7595)	PK – LK	1.0423 (1.2780, 0.8067)	<0.001
16	RIS-KET	1.0416 (0.6609, 1.4222)	PK – RK	1.3796 (1.6152, 1.1439)	<0.001
16	PLA-SAL	-0.1072 (-0.4879, 0.2735)			

[1]Abbreviations: ROI = regions of interest, N = the number of subjects, LS = least square, CI = confidence interval, PS = Placebo + Saline, PK = Placebo + Ketamine, RK = Risperidone + Ketamine, LK = Lamotrigine + Ketamine.

[2]ROIs: Anterior cingulate cortex, Supragenual paracingulate gyrus, Thalamus, Posterior cingulate cortex, Supplementary motor area, Insula left, Insula right, Operculum left, Operculum right, Precuneus, Medial occipital lobes.

JPET Fast Forward. Published on January 31, 2013 as DOI: 10.1124/jpet.112.201665
This article has not been copyedited and formatted. The final version may differ from this version.

Table 2: Comparison of LS mean difference across all positive-responding coordinate ROIs[1,2]

			Contrast		
N	**Treatment**	**LS Mean (95% CI)**	**Paired comparison**	**Difference (95% CI)**	**p**
16	PLA-KET	3.2793(2.7313, 3.8273)	PK – PS	3.4505 (2.9890, 3.9120)	<0.001
16	LAM-KET	1.9209(1.3728, 2.4689)	PK – LK	1.3584 (1.8199, 0.8969)	<0.001
16	RIS-KET	1.5085(0.9605, 2.0565)	PK – RK	1.7708 (2.2323, 1.3093)	<0.001
16	PLA-SAL	-0.1712(-0.7192, 0.3768)			

[1]Abbreviations: ROI = regions of interest, N = the number of subjects, LS = least square, CI = confidence interval, PS = Placebo + Saline, PK = Placebo + Ketamine, RK = Risperidone + Ketamine, LK = Lamotrigine + Ketamine.

[2]ROIs: anterior cingulate cortex, medial prefrontal cortex, right dorsolateral prefrontal cortex, right ventrolateral prefrontal cortex, left parahippocampal gyrus, right parahippocampal gyrus, mid-cingulate cortex.

JPET Fast Forward. Published on January 31, 2013 as DOI: 10.1124/jpet.112.201665
This article has not been copyedited and formatted. The final version may differ from this version.

Table 3: Comparison of LS mean difference across the two negative-responding coordinate ROIs[1,2].

			Contrast		
N	**Treatment**	**LS Mean (95% CI)**	**Paired comparison**	**Difference (95% CI)**	**p**
16	PLA-KET	-5.0929 (-6.7774, -3.4084)	PK – PS	-4.9542 (-6.6589, -3.2495)	<0.001
16	LAM-KET	-3.3569 (-5.0414, -1.6725)	PK – LK	-1.7360 (-0.0313, -3.4407)	0.046
16	RIS-KET	-0.2679 (-1.9523, 1.4166)	PK – RK	-4.8251 (-3.1204, -6.5297)	<0.001
16	PLA-SAL	-0.1387 (-1.8232, 1.5458)			

[1]Abbreviations: ROI = regions of interest, N = the number of subjects, LS = least square, CI = confidence interval, PS = Placebo + Saline, PK = Placebo + Ketamine, RK = Risperidone + Ketamine, LK = Lamotrigine + Ketamine.

[2]ROIs: Subgenual cingulate cortex coordinates from (De Simoni et al., 2012) and (Deakin et al., 2008).

JPET Fast Forward. Published on January 31, 2013 as DOI: 10.1124/jpet.112.201665
This article has not been copyedited and formatted. The final version may differ from this version.

Table 4: Classification performance for the models trained on a *static* contrast and tested on three of the contrasts. The nomenclature p(y=*PLA-KET*|$x_{*\text{-KET}}$) implies the probability of belonging to the PLA-KET class given conditions where ketamine has been administered but the pretreatment (* - PLA, RIS, LAM) varies. Similarly, p(y=*PLA-KET*|$x_{\text{PLA-SAL}}$) denotes the probability of belonging to the ketamine class given the PLA-SAL condition and is reported as the mean ± standard deviation.

	Training Contrast	Test Contrast PLA-SAL vs. PLA-KET	Test Contrast PLA-SAL vs. LAM-KET	Test Contrast PLA-SAL vs. RIS-KET
Accuracy	PLA-SAL vs. PLA-KET	100%	87.5%	75.0%
Sensitivity		100%	75.0%	50%
Specificity		100%	100%	100%
p(y=*PLA-KET*|$\mathbf{x}_{*\text{-KET}}$)		0.88 ± 0.14	0.58±0.56	0.49±0.34
p(y=*PLA-KET*|$\mathbf{x}_{\text{PLA-SAL}}$)		0.12±0.14	0.12±0.14	0.12±0.14

JPET Fast Forward. Published on January 31, 2013 as DOI: 10.1124/jpet.112.201665
This article has not been copyedited and formatted. The final version may differ from this version.

Figure 1

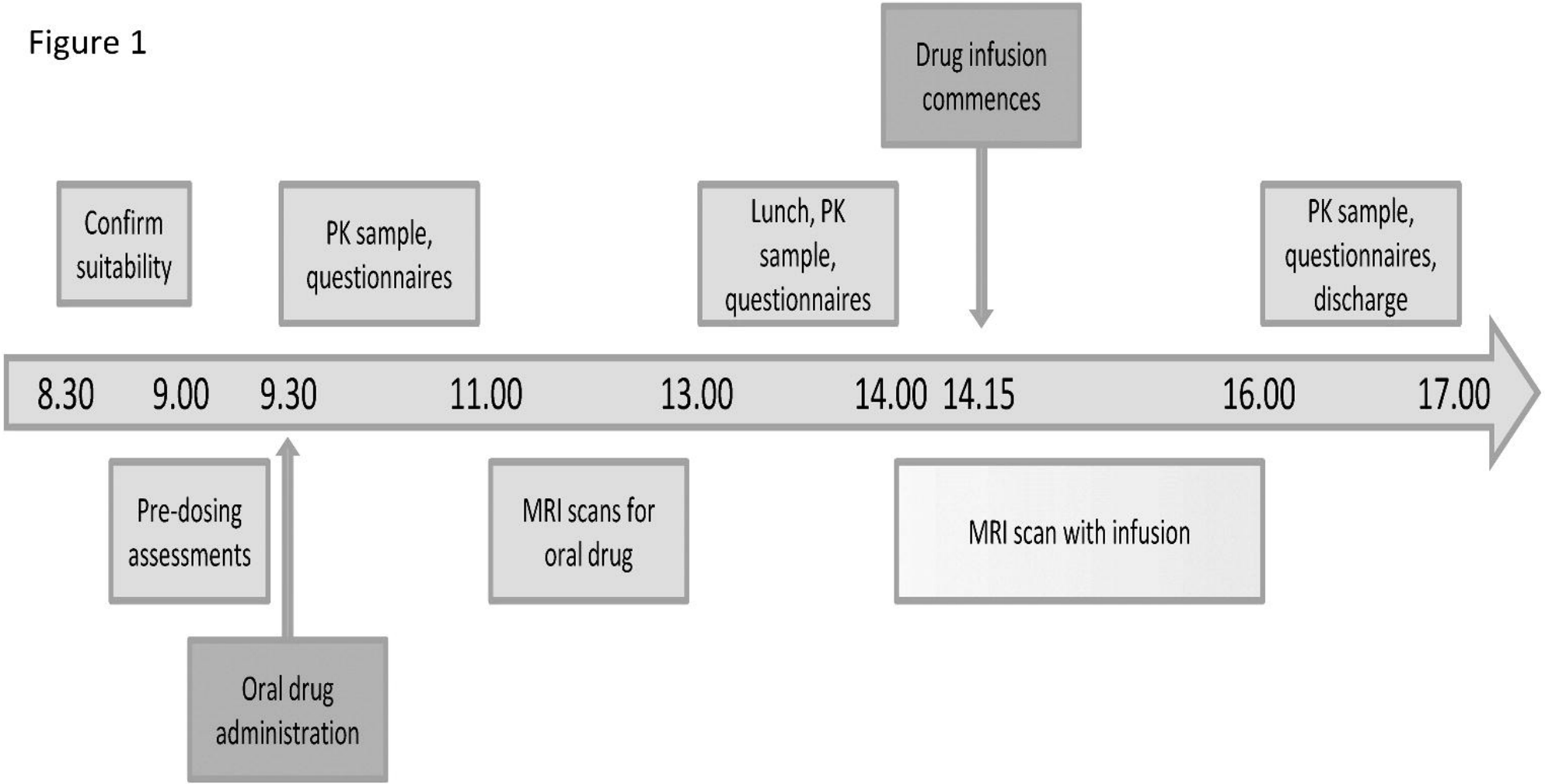
Drug infusion commences
Confirm suitability
PK sample, questionnaires
Lunch, PK sample, questionnaires
PK sample, questionnaires, discharge
8.30
9.00
9.30
11.00
13.00
14.00
14.15
16.00
17.00
Pre-dosing assessments
Oral drug administration
MRI scans for oral drug
MRI scan with infusion

Figure 2

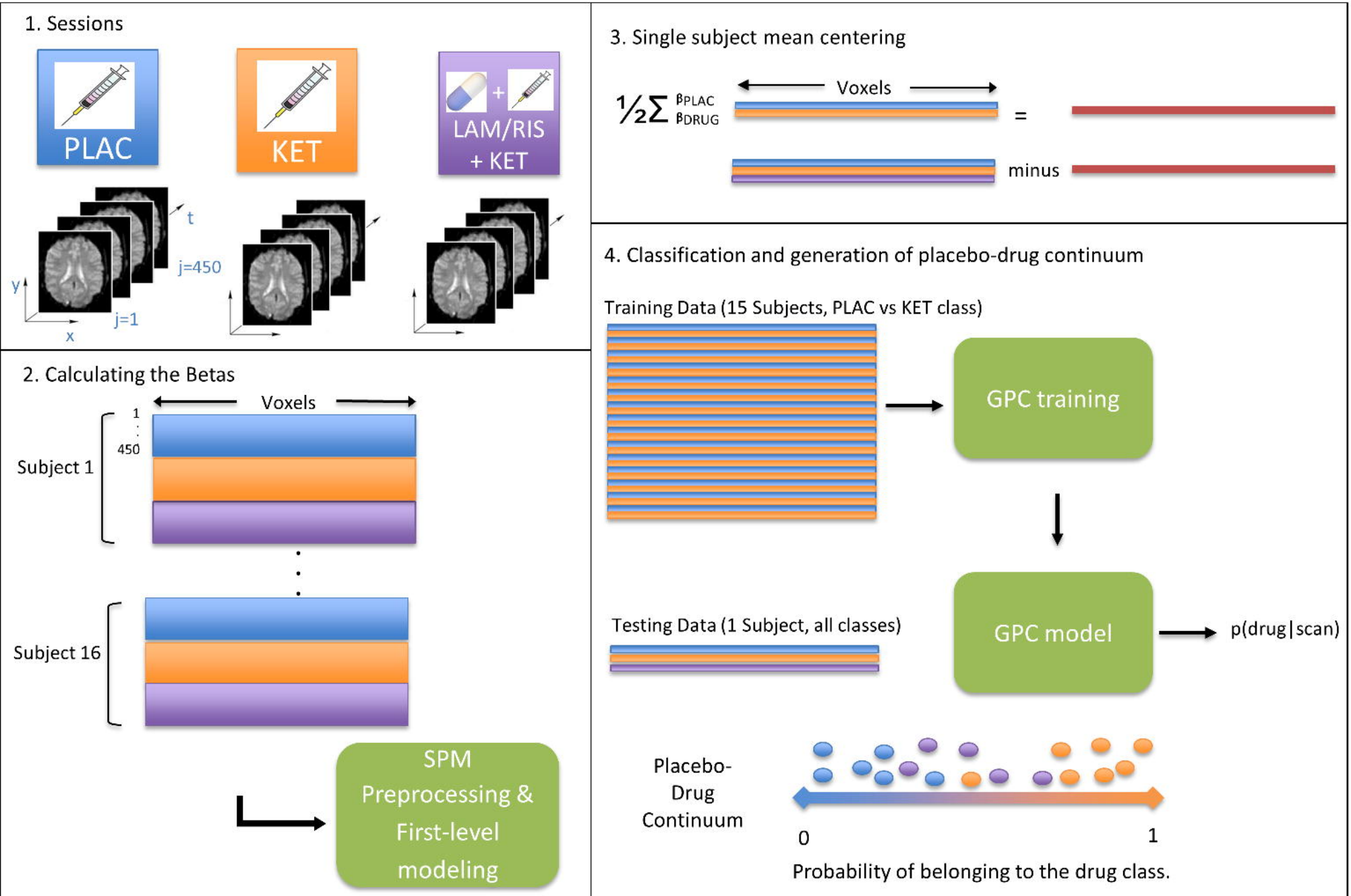
1. Sessions
PLAC
KET
LAM/RIS
+ KET
t
j=450
y
j=1
x
2. Calculating the Betas
Voxels
1
450
Subject 1
Subject 16
SPM
Preprocessing &
First-level
modeling
3. Single subject mean centering
½Σ βPLAC βDRUG
Voxels
=
minus
4. Classification and generation of placebo-drug continuum
Training Data (15 Subjects, PLAC vs KET class)
GPC training
Testing Data (1 Subject, all classes)
GPC model
p(drug|scan)
Placebo-
Drug
Continuum
0
1
Probability of belonging to the drug class.

Figure 3

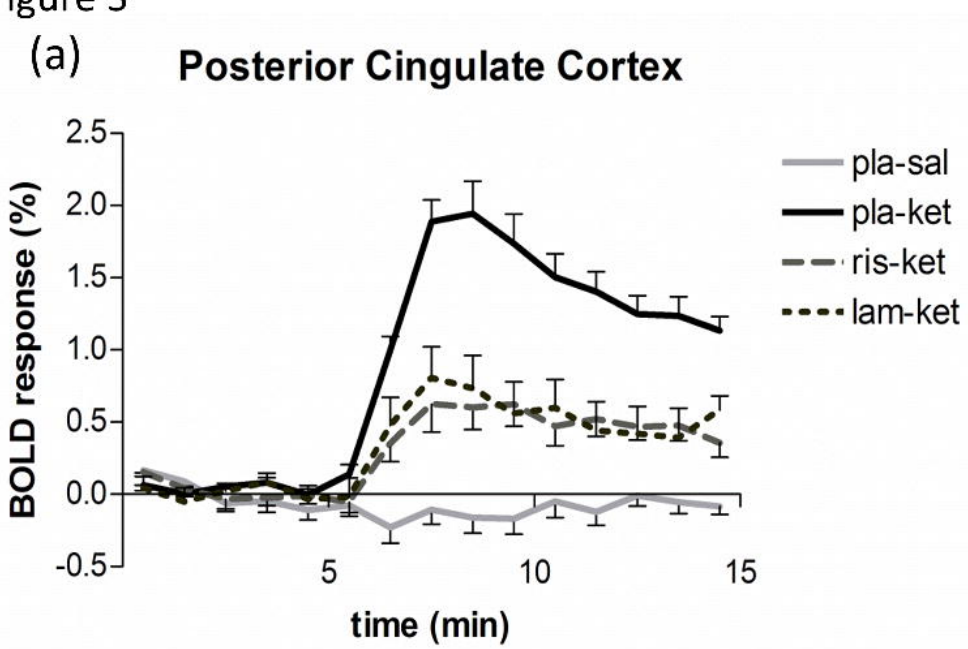
(a)
Posterior Cingulate Cortex
BOLD response (%)
2.5
2.0
1.5
1.0
0.5
0.0
-0.5
5
10
15
time (min)
pla-sal
pla-ket
ris-ket
lam-ket

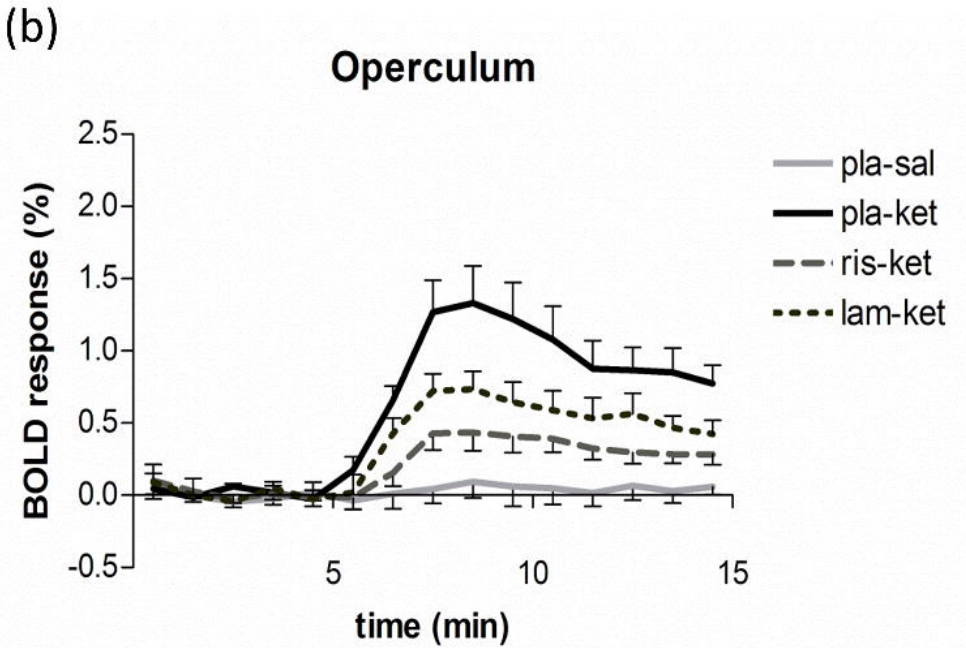
(b)
Operculum
BOLD response (%)
2.5
2.0
1.5
1.0
0.5
0.0
-0.5
5
10
15
time (min)
pla-sal
pla-ket
ris-ket
lam-ket

Figure 4

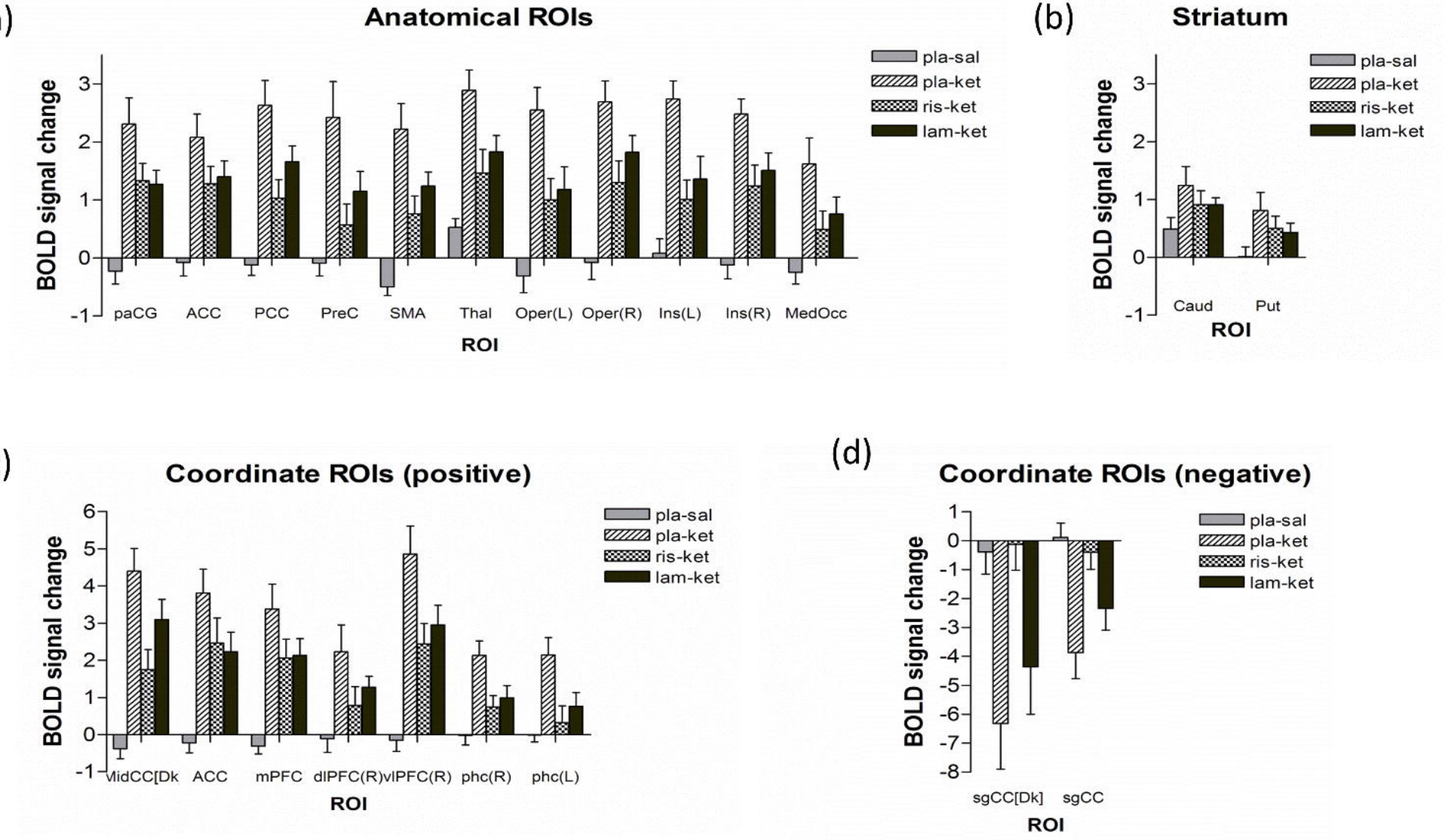
(a)
Anatomical ROIs
BOLD signal change
3
2
1
0
-1
paCG
ACC
PCC
PreC
SMA
Thal
Oper(L)
Oper(R)
Ins(L)
Ins(R)
MedOcc
ROI
pla-sal
pla-ket
ris-ket
lam-ket
(b)
Striatum
BOLD signal change
3
2
1
0
-1
Caud
Put
ROI
pla-sal
pla-ket
ris-ket
lam-ket
(c)
Coordinate ROIs (positive)
BOLD signal change
6
5
4
3
2
1
0
-1
MidCC[Dk
ACC
mPFC
dlPFC(R)
vlPFC(R)
phc(R)
phc(L)
ROI
pla-sal
pla-ket
ris-ket
lam-ket
(d)
Coordinate ROIs (negative)
BOLD signal change
1
0
-1
-2
-3
-4
-5
-6
-7
-8
sgCC[Dk]
sgCC
ROI
pla-sal
pla-ket
ris-ket
lam-ket

Figure 5

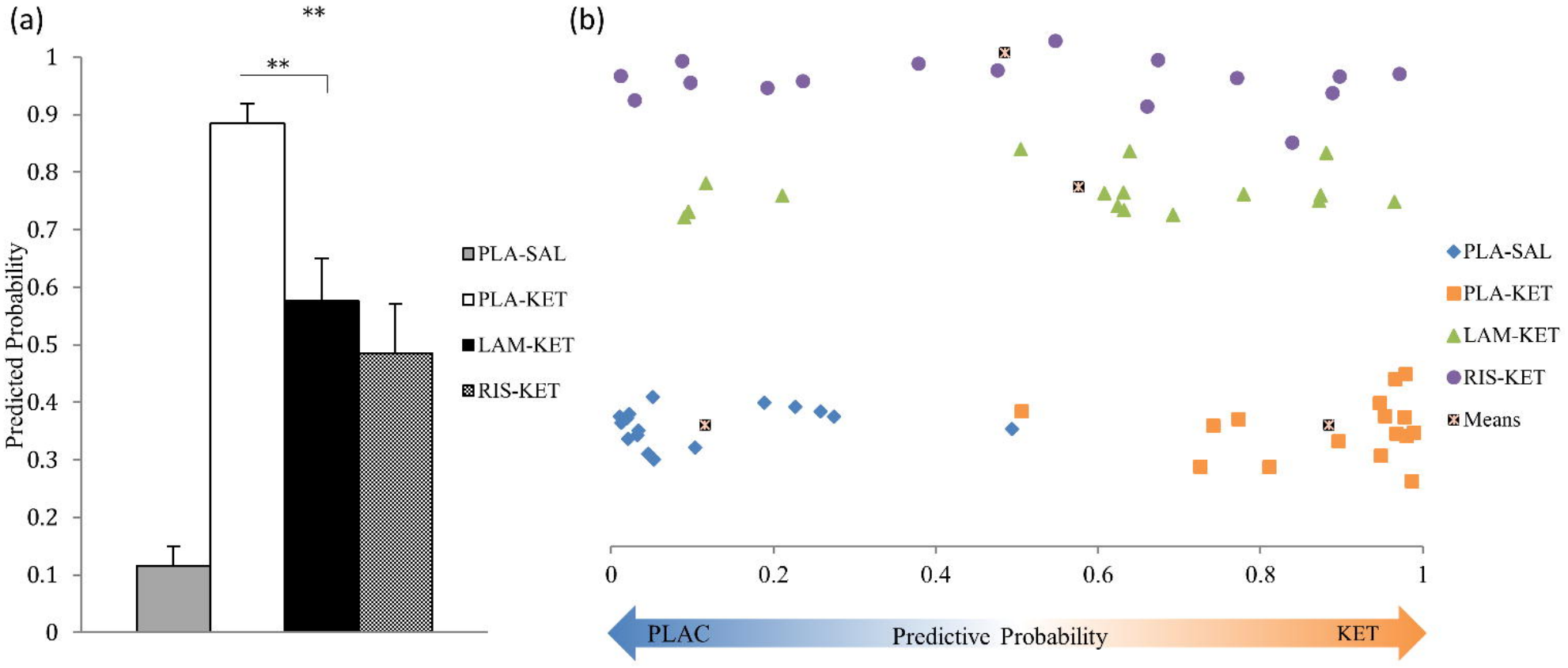
(a)
**
**
Predicted Probability
1
0.9
0.8
0.7
0.6
0.5
0.4
0.3
0.2
0.1
0
PLA-SAL
PLA-KET
LAM-KET
RIS-KET
(b)
PLA-SAL
PLA-KET
LAM-KET
RIS-KET
Means
0
0.2
0.4
0.6
0.8
1
PLAC
Predictive Probability
KET

Figure 6

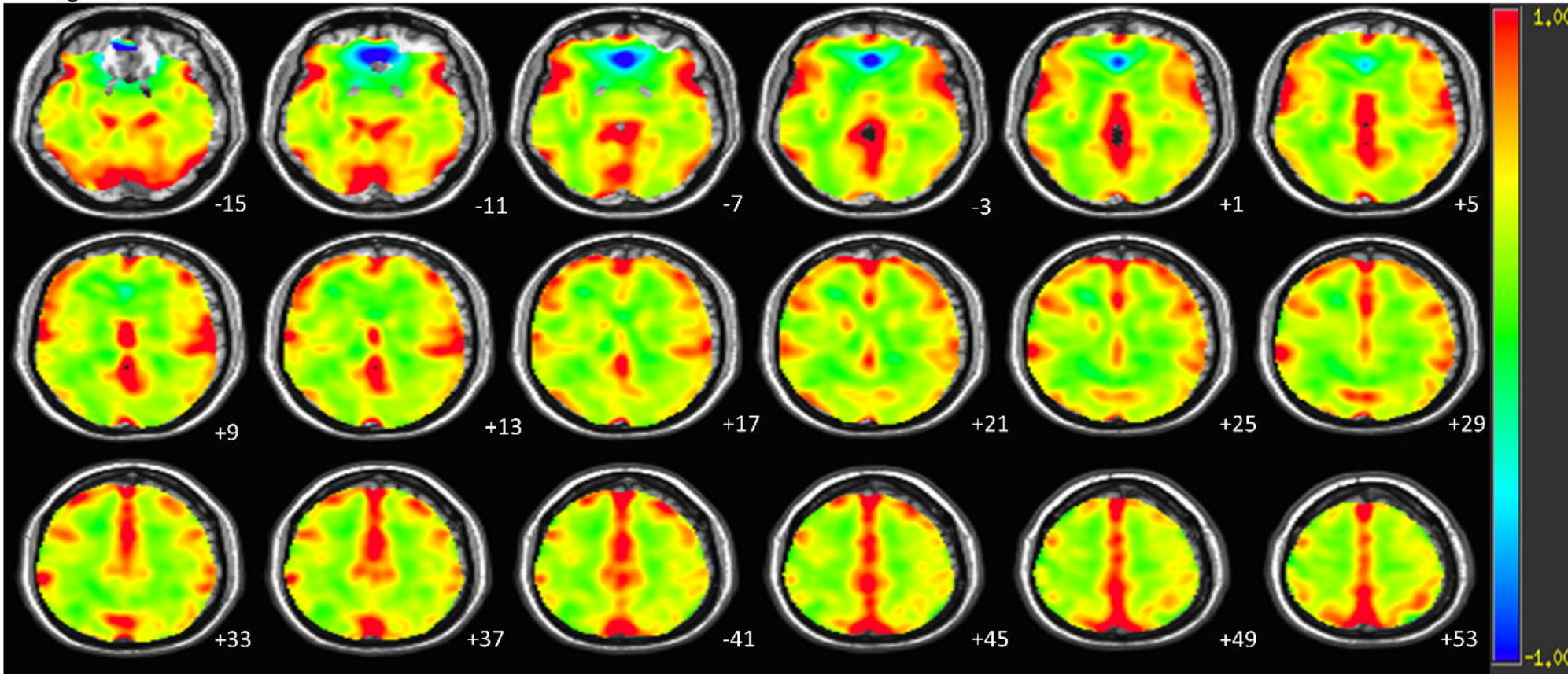

Journal of Pharmacology and Experimental Therapeutics

Supplementary Material for:

Quantifying the attenuation of the ketamine phMRI response in humans: a validation using antipsychotic and glutamatergic agents.

O.M. Doyle , S. De Simoni, A.J. Schwarz, C. Brittain, O.G. O'Daly, S.C.R Williams and M.A. Mehta .

METHODS

ROI definitions for univariate analysis

Regions of interest for the primary univariate analysis were pre-specified and based on brain regions strongly responding to the ketamine challenge in an independent cohort of subjects (De Simoni et al., 2012) and on the previously published report (Deakin et al., 2008). Both anatomical regions (based on an atlas) and smaller spheres centred on specific coordinates were defined as follows.

Harvard-Oxford probabilistic atlas structures, thresholded at 25% were anterior cingulate cortex, supragenual paracingulate cortex, thalamus, posterior cingulate cortex, supplementary motor area, left anterior insula, right anterior insula, left operculum, right operculum, precuneus and medial occipital lobes. The following modifications were made: the supragenual paracingulate cortex ROI was derived from the paracingulate gyrus atlas structure by retaining voxels only with MNI z-coordinate Z>0mm; the anterior insula masks were created from the atlas insula structure by retaining voxels with MNI y-coordinate Y>0mm, since the strongest BOLD response to ketamine was previously observed in the anterior portion (De Simoni et al., 2012). In addition, we also specified caudate and putamen atlas regions (bilaterally) in order to test for D_2 receptor related effects of risperidone.

We also pre-specified 9 smaller ROIs as 10mm diameter spheres centred on coordinates corresponding to local maxima in the response to ketamine in previous studies. Seven of these captured peak positive BOLD changes and were centred on voxels of peak response in the anterior cingulate cortex (MNI coordinates (-2,28,28)), medial prefrontal cortex (0,24,48), right dorsolateral prefrontal cortex (50,20,34), right ventrolateral prefrontal cortex (42,26,-8) and both left (-28,-32,-18) and right (22,-36,-14) parahippocampal gyri. The remaining ROIs captured negative responses in the subgenual cingulate region (2,30,-6) based on the peak negative response reported in (De Simoni et al., 2012), and the negative peak (3,39,-21) in the ventromedial prefrontal cortex reported in (Deakin et al., 2008).

Gaussian Process classification

Gaussian processes (GP) can be used to specify distributions over functions without having knowledge of the specific functional form (Rasmussen et al., 2006). A GP is a stochastic process $f(\boldsymbol{x})$ over a multidimensional input space (here, each voxel is considered as a unique dimension), $\boldsymbol{x}$ parameterised by a mean $m(\boldsymbol{x})$ and covariance function $k(\boldsymbol{x}, \boldsymbol{x}')$. Here, GP learning is achieved using Bayesian inference. This involves a three step process; first, a GP prior is placed on a latent function **f** that qualitatively relates the data to the output labels **y** (which correspond to the drug conditions), the output of this latent function is then mapped onto [0 1] using a link function. Second, the data are observed and third, a posterior distribution over **f** is computed that refines the prior by incorporating evidence from the observations.

By placing a GP prior over the parameters of the model we restrain the solution in some particular manner, i.e. regularisation. Regularisation helps alleviate the curse of dimensionality whereby the dimensionality of the data (number of voxels) greatly exceeds the number of samples (scans, or beta maps in this case). For the GP prior, the mean and covariance functions must be specified. In most applications, we will not have any knowledge about mean of the prior and so it is taken to be zero (Bishop, 2006) so, $m(\boldsymbol{x}) \equiv 0$. The role of the covariance function of the GP prior is similar to that of kernels, widely used in machine learning. The covariance function defines the covariance between the function at two different time points or indices. Its specification is important because it encodes our assumptions about the function we wish to learn for example, linear, smooth, etc. Additionally, the covariance function also defines the notion of nearness or similarity in the data, i.e. the training data that are closest to a test point should be informative about the prediction at that point. Several formations for the covariance function are presented in (Rasmussen et al., 2006).

In this work, the covariance function takes the form,

$$\boldsymbol{K} = \boldsymbol{X}\boldsymbol{X}^{\boldsymbol{T}}.$$

where $\boldsymbol{X}$ represents whole brain beta maps constructed from the phMRI data and is created by intitially horizontally concatenating the beta values for each voxel into a vector with dimensions $Nx1$ where N is the number of voxels for analysis and finally the data from the training subjects is

vertically concatenated to give a matrix $\boldsymbol{X}$ with dimensions *NxM* and where M is the number of subjects in the training set.

Linear GP classification (GPC), implemented here, can be considered a Bayesian extension of logistic regression where the probability of membership of class 1 is derived by *squashing* the output of a regression model $\boldsymbol{f}$ into a class probability using a link function, i.e. $(y_* = 1|\boldsymbol{X}, \boldsymbol{y}, \boldsymbol{x}_*) = \sigma(f_*)$, where $p(y_* = 1|\boldsymbol{X}, \boldsymbol{y}, \boldsymbol{x}_*)$ is the predicative probability of the test case $\boldsymbol{x}_*$ belonging to the class labelled as 1, σ is the link function, f_* is the latent function and y_* is the label for the test case. The latent function plays the role of a *nuisance function,* i.e. we do not observe the values of $\boldsymbol{f}$ directly but rather the values of σ for particular test cases. Here, we used the probit likelihood function: σ(z) = Φ(z) = $\int_{-\infty}^{z} \aleph(u|0,1)du$.

Inference is divided into two steps. First, the distribution of the latent variable corresponding to a test case is computed,

$$p(f_*|\boldsymbol{X}, \boldsymbol{y}, \boldsymbol{x}_*) = \int p(f_*|\boldsymbol{X}, \boldsymbol{x}_*, \boldsymbol{f})p(f|\boldsymbol{X}, \boldsymbol{y})d\boldsymbol{f},$$

where $p(f|\boldsymbol{X}, \boldsymbol{y})$ is the posterior over the latent variables. This distribution can then be used to produce a probabilistic prediction,

$$p(y_* = 1|\boldsymbol{X}, \boldsymbol{y}, \boldsymbol{x}_*) = \int \Phi(f_*)p(f_*|\boldsymbol{X}, \boldsymbol{y}, \boldsymbol{x}_*)df_*.$$

For classification, the posterior over the latent variables is non-Gaussian and hence the likelihood $p(f_*|\boldsymbol{X}, \boldsymbol{y}, \boldsymbol{x}_*)$ is analytically intractable. Therefore, we employ an analytic approximation of the integrals. Here, this is achieved using expectation propagation (Rasmussen et al., 2006).

Multivariate maps using GPC

For neuroimaging applications, in order to visual the spatial pattern which drives the classification model we generate multivariate maps. To achieve this each training sample is weighted by the mean of the latent function at each training point $\boldsymbol{x}_i$ (a single beta map from the training set):

$$\boldsymbol{g} = \sum_{i=1}^{m} \mu_i \boldsymbol{x}_i = \boldsymbol{X}^T \boldsymbol{m}.$$

The per-voxel measure $\boldsymbol{g}$ describes the distribution of the two classes with respect to one another. The training samples with the highest μ_i are the most confidently classified. Thus, training samples contribute to $\boldsymbol{g}$ in proportion to how representative they are of their respective class. This approach to

multivariate mapping has been shown, qualitatively, to produce maps that bear a strong resemblance to statistical parametric maps (SPMs) (Marquand et al., 2010).

GPC was implemented in MATLAB using a customised version of the Gaussian Process for Machine Learning toolbox, (www.gaussianprocess.org/gpml).

Physiological Measurements

Table S1 describes the vascular and blood pressure effects during all treatment conditions at four time-points during the testing day. No significant differences were found between treatment conditions for any measurement.

Table S1: Cardiovascular Measurements (Mean +/- Standard Error)

		Blood Pressure (mmHg)		Heart Rate (beats/min)
		Supine Systolic	**Supine Diastolic**	**Supine**
PLA-SAL	**Admission**	118.4 (2.1)	70.1 (1.9)	63.0 (2.5)
	1h30 Post Oral Dose	116.8 (2.0)	70.4 (2.0)	52.4 (1.8)
	4h Post Oral Dose	120.7 (1.9)	66.1 (2.1)	59.7 (2.1)
	Discharge	120.7 (2.2)	68.4 (2.2)	55.6 (2.2)
PLA-KET	**Admission**	115.9 (1.9)	69.2 (1.1)	61.7 (2.6)
	1h30 Post Oral Dose	116.7 (2.2)	68.9 (1.6)	53.8 (2.0)
	4h Post Oral Dose	119.5 (2.3)	66.2 (1.8)	57.0 (2.2)
	Discharge	122.1 (2.2)	72.7 (2.1)	57.2 (2.0)
RIS-KET	**Admission**	120.1 (2.1)	71.1 (1.7)	62.9 (2.0)
	1h30 Post Oral Dose	115.9 (2.8)	66.8 (1.8)	57.9 (1.7)
	4h Post Oral Dose	123.2 (2.8)	68.3 (1.9)	65.1 (1.9)
	Discharge	122.5 (2.8)	69.9 (1.5)	61.7 (2.3)
LAM-KET	**Admission**	119.4 (2.2)	71.6 (1.1)	63.4 (1.8)
	1h30 Post Oral Dose	118.2 (2.7)	69.4 (1.4)	56.4 (2.1)
	4h Post Oral Dose	120.3 (2.8)	65.9 (1.5)	61.7 (2.1)
Dis	**charge**	122.6 (2.8)	71.7 (1.9)	58.4 (1.8)

Subjective Scores

Table S2 specifies 6 questionnaire items from three different clinical scales that were determined in a previous study on a different cohort of subjects to most reliably and sensitively capture the subjective effects of ketamine at the dose and schedule administered (1). This provides a rapid means of tracking the subjective state of the subjects in the scanner during the imaging procedure.

Table S 2: Brief questionnaire to index subjective response to ketamine. The visual analogue scale (VAS) comprised a 15cm line divided in 100 points. The PSI and CADDS scales comprised a numeric scale from 0 to 3.

Item Sca	**le**
Alert – Drowsy	VAS
Muzzy – Clear Headed	VAS
Do you feel more sensitive to light or the colour or brightness of things?	PSI
Is your experience of time unnaturally fast or slow?	PSI
Do you feel as though your head, limbs, or body have somehow changed?	PSI
Do things seem unreal to you as if you are in a dream?	CADDS

RESULTS

Univariate voxelwise analysis

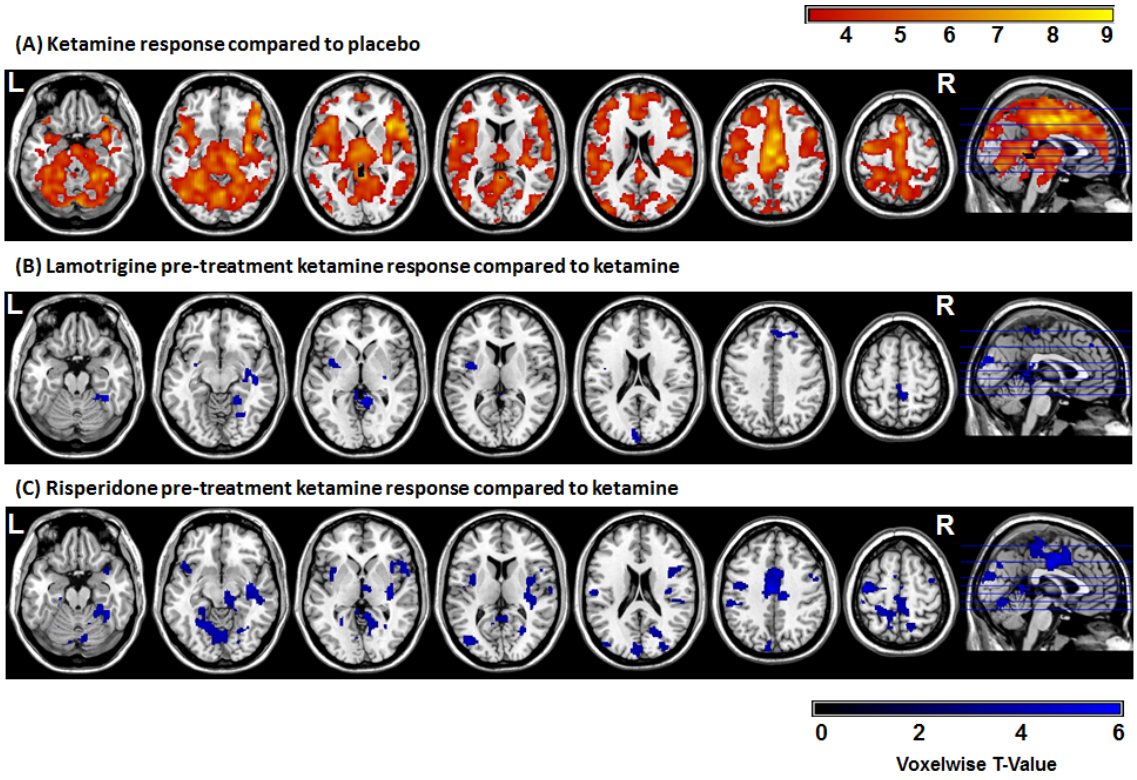

Figure S 1: Mass univariate contrasts of the ketamine response compared to placebo (A), lamotrigine pre-treatment ketamine response (B) and risperidone pre-treatment ketamine response (C). Increases in activation (red-yellow) represent areas that respond to a greater extent to ketamine compared to placebo. Decreases in activation (blue) represent areas that respond to ketamine administration but are attenuated by either lamotrigine or risperidone pre-treatment. T- maps are thresholded at whole brain cluster significance of $P<0.05$ corrected for multiple comparisons, voxel threshold of $P<0.001$.

Additional GPC analyses

In order to investigate if LAM and RIS pre-treatment attenuated the distributed regions that defined the response to ketamine we performed two additional analyses to discriminate LAM-KET from PLA-KET and RIS_KET from PLA-KET. Specifically, the GPC was trained and tested on the LAM-KET versus PLA-KET images and, separately, on the RIS-KET versus PLA-KET images. The results for both of these analyses can be seen in Table S3. Both classifiers performed above chance and the predicted probabilities of the pre-treatment scans being PLA-KET was low in both cases. In addition the maps (Figures S3 and S4) show that the discrimination pattern for the pre-treatment scans was similar to the pattern for PLA-SAL vs PLA-KET. This allows us to conclude that both LAM and RIS globally attenuated the KET response.

The performance of the classifier trained and tested on the RIS-KET versus PLA-KET contrast (81%) outperformed the LAM-KET versus PLA-KET (69%). In conjunction with the lower predicted probabilities of the pre-treatment scans belonging to the PLA-KET class ($p=0.004$ and $p=0.00002$ for the LAM-KET and RIS-KET classes respectively using a Wilcoxon signed-ranked matched pairs test), implies that the RIS-KET condition more closely resembles the PLA-SAL response than does the LAM-KET condition.

Table S3: Classification performance of the pre-dosed drug conditions versus the ketamine condition.

	Training Contrast	Test Contrast PLA-KET vs. LAM-KET	Training Contrast	Test Contrast PLA-KET vs. RIS-KET
Accuracy	PLA-KET vs. LAM-KET	68.8%	PLA-KET vs. RIS-KET	81.3%
Sensitivity		68.8%		81.3%
Specificity		68.8%		81.3%
$p(y=PLA\text{-}KET\|\mathbf{x}_{PLA\text{-}KET})$		0.64±0.22		0.73±0.20
$p(y=PLA\text{-}KET\|\mathbf{x}_{*\text{-}KET})$		0.36±0.22		0.27±0.20

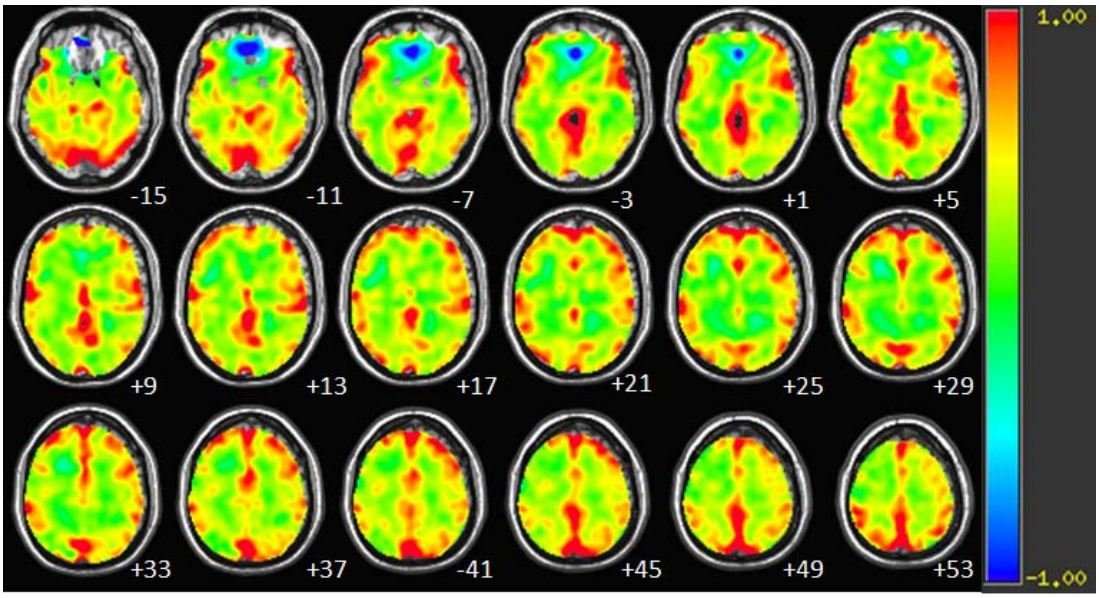

Figure S2: Multivariate map (g-map) from the GPC which contrasts PLA-KET (class label: +1) and LAM-KET (class label: -1). A positive g-map coefficient for a particular voxel indicates a higher overall beta score for the PLA-KET class (+1) and similarly, a negative g-map coefficient indicates a higher overall beta score for the LAM-KET class (-1).). The right hand side of each image corresponds to the participants' right side with the transaxial slice numbers in MNI coordinates (z-axis) shown in white.

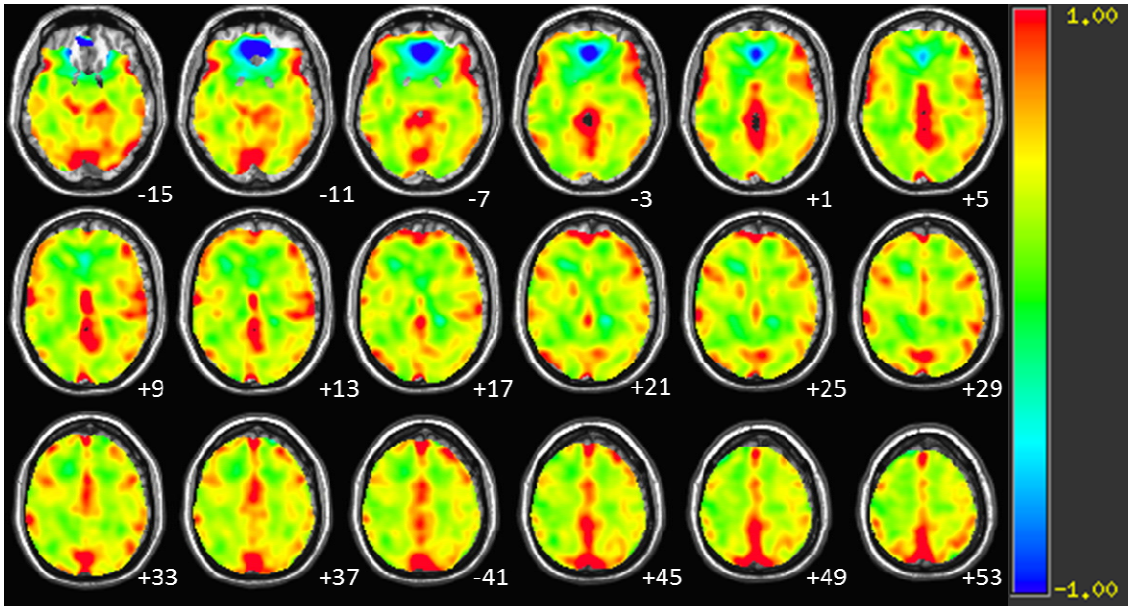

Figure S3: Multivariate map (g-map) from the GPC which contrasts PLA-KET (class label: +1) and RIS-KET (class label: -1). A positive g-map coefficient for a particular voxel indicates a higher overall beta score for the PLA-KET class (+1) and similarly, a negative g-map coefficient indicates a higher overall beta score for the RIS-KET class (-1).). The right hand side of each image corresponds to the participants' right side with the transaxial slice numbers in MNI coordinates (z-axis) shown in white.

To directly contrast LAM-KET and RIS-KET we trained and tested the GPC on their respective scans. This resulted in a classification accuracy of 56% ($p>0.05$). This implies that the patterns representing both pre-treated scans could not be discriminated by the GPC.

Subjective Scores

The post- vs. pre-ketamine infusion responses for the two visual analogue scale (VAS) items from the brief questionnaire are summarised in Figures S5 and S6. For the alert-drowsy VAS scale, a trend to increased score (more drowsy) is evident for all conditions, although a significant difference (tested with a paired Wilcoxon signed rank sum test) was observed for the PLA-KET condition only (Figure S4). In addition, subjects tended to score higher on this scale when pre-treated with RIS as opposed to LAM or PLA, $p = 0.0094$ and $p = 0.0044$, respectively. For the muzzy-clear VAS scale, again a similar trend was observed in all conditions, with significant decreases (corresponding to more muzzy) found for all ketamine infusion conditions but not the PLA-SAL condition (Figure S6). Subjects tended to score lower on the muzzy-clear scale ($p=0.0054$) following pre-treatment with risperidone as compared to placebo pre-treatment in the control arm of the study. The similarity in the direction of the effect between pre- and post-infusion conditions in all treatment arms demonstrates that ketamine-induced changes in subjective ratings were not attenuated by lamotrigine or risperidone.

In addition, four statements were also presented and the participants scored the this statement on a scale of 0 to 5 with 0 implying the effect was not experienced and 5 implying that the effect was experienced very strongly (Table S4). For these scales, most participants scored zero and so scores of greater than one were sparse across subjects. These subtle effects may be unexpected as these particular scales were chosen on the basis of their sensitivity to the effects of ketamine in a previous cohort. Nonetheless, this may simply be due to differences in the time (post-ketamine infusion) at which these were acquired. Due to the nature of the data we did not apply any statistical tests but instead we present the median, interquartile range, mean and standard deviation so give an insight into the data. Overall, in comparison to the imaging data, subjective ratings appear less sensitive to the modulation of the ketamine response by lamotrigine and risperidone.

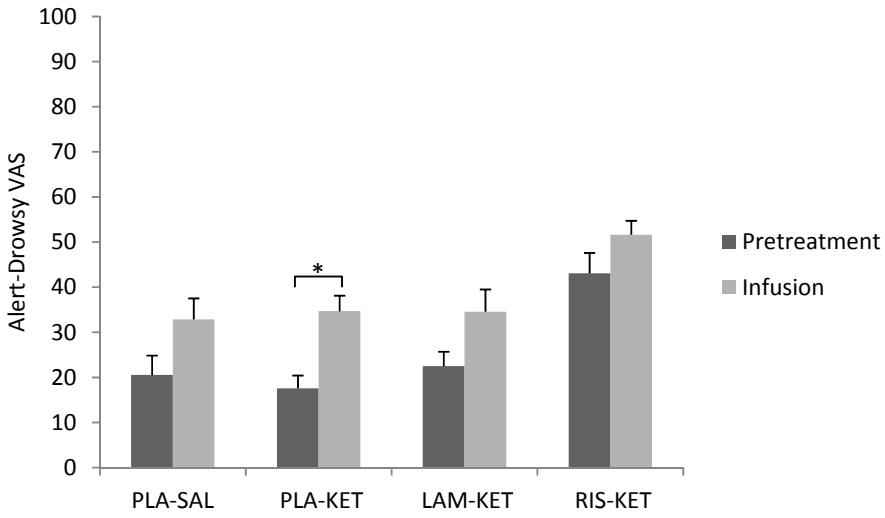

Figure S4: Visual analogue scales (VAS) for alert to drowsy across all four sessions following pretreatment and following infusion. *: $p < 0.05$

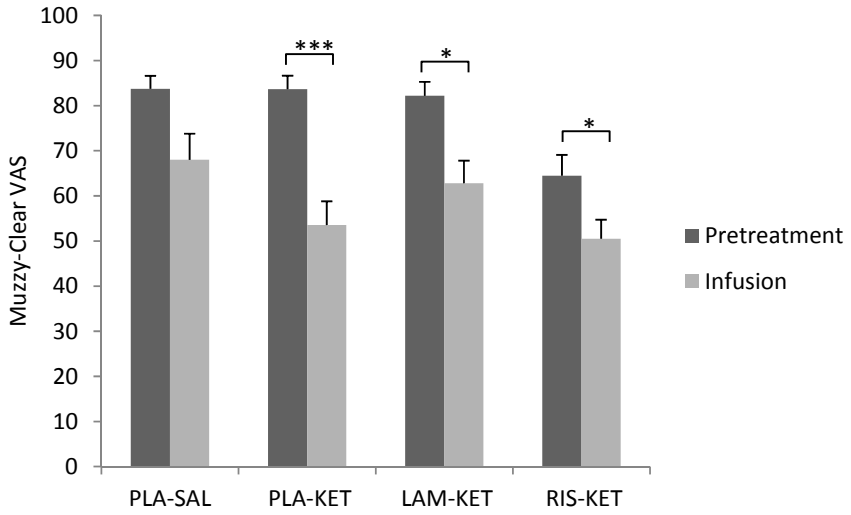

Figure S5: Visual analogue scales (VAS) for muzzy (muddled and fuzzy) to clear across all four sessions following pretreatment and following infusion. *: $p < 0.05$, ***: $p < 0.001$.

Table S4: Subjective scores acquired after pre-treatment and after infusion across all four sessions. All questions are answered using a scale of zero to five where zero implies the effect in the statement was not experienced. Here, "PLA", "PLA", "LAM" and "RIS" refer to the pre-infusion questionnaires for the immediately adjacent conditions.

You feel more sensitive to light or the colour or brightness of things. (0 to 5)								
	PLA	PLA-SAL	PLA	PLA-KET	LAM	LAM-KET	RIS	RIS-KET
Median	0	0	0	0	0	0	0	0

IQR	0	0	0	1	0	0	0	1
Mean	0.07	0.13	0.07	0.44	0	0.31	0.01	0.56
Std Dev	0.26	0.35	0.258	0.63	0	0.70	0.26	0.81
Your experience of time is unnaturally fast or slow. (0 to 5)								
	PLA	PLA-SAL	PLA	PLA-KET	LAM	LAM-KET	RIS	RIS-KET
Median	0	0	0	0	0	0	0	0
IQR	0	0	0	1	0	1	0	1
Mean	0	0.07	0	0.38	0.06	0.50	0.07	0.44
Std Dev	0	0.26	0	0.50	0.25	0.82	0.26	0.81
Do things seem unreal to you as if you are in a dream. (0 to 5)								
	PLA	PLA-SAL	PLA	PLA-KET	LAM	LAM-KET	RIS	RIS-KET
Median	0	0	0	0	0	0	0	0
IQR	0	0	0	1	0	0	0	0
Mean	0	0	0	0.31	0	0.25	0.07	0.06
Std Dev	0	0	0	0.48	0	0.58	0.26	0.25
You feel as though your head, limbs or body have somehow changed. (0 to 5)								
	PLA	PLA-SAL	PLA	PLA-KET	LAM	LAM-KET	RIS	RIS-KET
Median	0	0	0	0	0	0	0	0
IQR	0	0	0	0	0	1	0	0
Mean	0	0	0	0.25	0.06	0.31	0	0.13
Std Dev	0	0	0	0.58	0.25	0.48	0	0.50

Correlations between PK and phMRI responses

For the KET conditions, no significant correlations between ketamine plasma levels at 15 mins or 75 mins and the BOLD phMRI changes in the specified ROIs were observed (Spearman's Rho = -0.34 – 0.45, NS). Similarly, no significant correlations were found between ketamine plasma concentrations at 15 minutes and the predicted probabilities from the GPC (Spearman's Rho = -0.033 – 0.30, NS). No significant correlations between risperidone or lamotrigine exposure (AUC [0-4.5h]) and either the BOLD phMRI changes in the specified ROIs in the univariate analysis or predictive probabilities from the multivariate analysis were observed.

Bishop CM (2006) *Pattern recognition and machine learning*. Springer, New York.

De Simoni S, Schwarz AJ, O'Daly OD, S. S, Zelaya FO, Williams SCR and Mehta MA (2012) Test-retest reliability of the BOLD pharmacological MRI response to ketamine in healthy volunteers. *NeuroImage* **In press**.

Deakin JF, Lees J, McKie S, Hallak JE, Williams SR and Dursun SM (2008) Glutamate and the neural basis of the subjective effects of ketamine: a pharmaco-magnetic resonance imaging study. *Archives of general psychiatry* **65**:154-164.

Marquand A, Howard M, Brammer M, Chu C, Coen S and Mourao-Miranda J (2010) Quantitative prediction of subjective pain intensity from whole-brain fMRI data using Gaussian processes. *NeuroImage* **49**:2178-2189.

Rasmussen CE, Williams CKI and Books24x7 Inc. (2006) Gaussian processes for machine learning, in, MIT Press, Cambridge, Mass.